11-20-2015

Optofluidic Spectroscopy Platform for Detection of Hemolysis

Edikan Archibong
University of South Florida, earchibong@mail.usf.edu

Optofluidic Spectroscopy Platform for Detection of Hemolysis

by

Edikan Archibong Ogunnaike

A dissertation submitted in partial fulfillment
of the requirements for the degree of
Doctor of Philosophy in Engineering Science
Department of Chemical and Biomedical Engineering
College of Engineering
University of South Florida

Major Professor: Anna Pyayt, Ph.D.
Lennox Hoyte, M.D.
Robert Frisina, Ph.D.
Sanjukta Bhanja, Ph.D.
Sylvia Thomas, Ph.D.
Valerie Whiteman, M.D.

Date of Approval:
October 28, 2015

Keywords: Microfiltration, pregnancy complications, blood testing, mobile medicine

DEDICATION

To God Almighty, I thank you. I am forever grateful for your grace, compassion, and mercy in sustaining me throughout the doctoral journey.

To my husband, Olusegun, and my daughter, Ima, life will never be complete or fun without your love and support. You both were my biggest advocate and we accomplished this feat together. I am looking forward to the next chapter of our lives.

To my parents, I am eternally grateful for your prayers and support. You both laid the foundation for me to succeed and this doctoral degree is dedicated to both of you. I owe a debt of gratitude that can never be repaid. To my dear sister, Mekutabasi, thank you for being there and for all that you do.

Lastly, I dedicate this dissertation to my mentors, Dr. Nelly Mateeva and Dr. Bernard Batson. You both sacrificed countless hours of your personal time to provide me guidance and support. I am here today because of your selflessness and your numerous investments in my future. I hope it paid off.

ACKNOWLEDGMENTS

I wish to express my gratitude and sincere thanks to several individuals throughout this dissertation who have directly and indirectly encouraged, supported, and provided resources for this degree to be realized.

Thank you Dr. Pyayt for the opportunity to work in your lab, I have learned a lot under your tutelage. I am grateful for your sacrifice. I know I will forever be in your heart as your first Ph.D. student!

I would like to thank Mr. (Dr.) Bernard Batson for his continuous support throughout my program. You are indeed the world's greatest mentor! As a result of your guidance, I have the privilege of expressing sincere appreciation to the Alfred P. Sloan Foundation Minority PhD (MPHD) program, NSF FGLSAMP Bridge to the Doctorate program (HRD #1139850), and the Florida Education Fund's McKnight Dissertation Fellowship program for their generous financial support.

My genuine appreciation is offered to Professors Sanjukta Bhanja, Sylvia W. Thomas, Robert Frisina, and Drs. Valerie Whiteman and Lennox Hoyte for serving as my committee members, and Professor Takshi for serving as my defense chair. I am grateful for your constant support and guidance. I would also like to recognize and express special thanks to Ms. Catherine for her unfailing guidance.

Lastly, I sincerely thank ALL my BD friends and lab mates, past and present. You all were instrumental in making my dream a reality.

TABLE OF CONTENTS

LIST OF TABLES

LIST OF FIGURES

ABSTRACT

In the United States alone, hundreds of millions of blood tests are performed annually, and a significant number of those tests are compromised due to hemolysis: e.g., 31% compromised in emergency rooms (inpatient) and 10% at blood banks, clinics, and other outpatient venues. Currently there is no way to reliably detect hemolysis without plasma separation. As a result, significant delays ensue, potentially negatively affecting patient diagnosis and treatment. In addition to *in vitro* hemolysis, which compromises the quality of blood tests, hemolysis can also occur *in vivo*. The *in vivo* occurrence of hemolysis is an indication of life-threatening complications. Being able to detect early signs of *in vivo* hemolysis would significantly improve outcomes for many patients, including pregnant women affected by HELLP (Hemolysis, Elevated Liver Enzymes, Low Platelet counts) syndrome. Therefore, there is a critical need to be able to detect hemolysis near the patient, immediately following the collecting of blood sample.

The goal of this research is to provide an alternative to the traditional testing of blood samples, which requires large volumes of blood, centrifugation, and bulky instrumentation. The proposed alternative hemolysis detection system is a simple miniature setup that produces test results in minutes. This miniature, near-patient sensor would improve patients' diagnosis, treatments, general satisfaction, and overall experience. The potential reduction of healthcare costs associated with hemolysis would be another significant benefit.

The technology demonstrated in this dissertation is based on a novel combination of microfluidics, spectroscopy, and optical-fiber sensing. The microfluidics provide the capability to handle small volumes of liquid and to filter particles from solution. Novel membrane fabrication and modular integration provides the means to characterize and culture the captured particles. Spectroscopy and optical fibers provide the means to characterize the filtrate. These capabilities can be used for not only the detection of hemolysis but also other biomedical applications. .

The first step in detecting hemolysis is to separate blood cells and other unwanted particulates from the plasma needed for optical analysis of concentration of hemoglobin. To that end, we focused initially on the problem of particle separation—specifically, within a microfabricated chamber with a custom-designed transparent membrane. To create a miniature microfluidic system capable of processing microliter blood samples, microelectromechanical systems (MEMS) fabrication techniques were required. The fabrication process included steps such as low-stress vapor deposition, photolithography, plasma, and wet etching. The resulting microdevice proved capable of filtering a variety of biological test fluids, including human lung fibroblast cancer cells from medium. The transparent membrane also allows for spectroscopic studies in broader applications, such as spectroscopic analysis or culturing of the cells retained on the filter. These capabilities were demonstrated using microbeads and cancer cells in solution.

Optical techniques are used to analyze the separated blood plasma for concentration of hemoglobin. To integrate spectroscopic capabilities with the above microfluidics system, an optical fiber–based miniature probe was attached to the microfabricated chamber. As proof of concept, this system was tested in an application that required the measurement of physiologically relevant concentrations of cobalamin (vitamin B_{12}). This application was used to

address human error in drug administration showing measurements of cobalamin concentration as an example drug that can be monitored. The clinical means range of concentrations is from 1 µg/ml to 1000 µg/ml. The achieved results showed measurements of concentrations between 1 µg /mL to 5 mg/mL to monitor the physiological range and potential overdose in microliter of volume.

This device has potential for numerous applications, ranging from single cell spectroscopy to measurements of glucose concentrations.

This integrated system was then applied to the detection of hemolysis. The complete system conducts optofluidic spectroscopy with the optical fiber probe connected to the microfabricated chamber, which locally filters out blood cells, and reliably determine amount of free hemoglobin with the need for centrifuging. The utility of the device was demonstrated by its accurate measurement of hemoglobin concentrations in blood plasma.

Finally, to apply the concept of the detection system to clinical condition with a reliable, and low-cost system, especially useful for developing countries, a smartphone-based technology, is proposed. This technology delivers ultra-fast results for the detection of early signs of HELLP syndrome and preeclampsia with the goal to decrease mortality and morbidity. The smartphone-based diagnostics is low cost, high speed of operation together with high accuracy. Detection of 1 mg/dL of free hemoglobin was achieved which is comparable to gold standard assay which are time consuming, difficult to operate and expensive.

This technology, in summary, integrates microfluidics with microfiltration and spectroscopic technology to conveniently separate and characterize blood plasma. The device can also provide important information about other complex biological samples. These measurements require only very small sample volumes.

CHAPTER 1: INTRODUCTION

1.1 Motivation

Prenatal conditions are the fourth leading cause of death in developing nations and also pose significant health risks in countries with high income [1]. Globally, preeclampsia and other hypertensive disorders of pregnancy are a leading cause of maternal and infant illness and death. By conservative estimates, these disorders are responsible for 76,000 maternal deaths and 500,000 infant deaths each year [2]. Preeclampsia can rapidly escalate to a dangerous complication known as HELLP (hemolysis, elevated liver enzymes, low platelets) syndrome. According to the Preeclampsia Foundation [2], the maternal mortality rate of HELLP syndrome has been reported to be as high as 25%. Overall perinatal mortality from HELLP Syndrome (stillbirth plus neonatal death) ranges from 7.7 to 60%. Among pregnant women in the United States, 5 to 8% develop preeclampsia. Clinical studies estimated that 15% of those women will develop evidence of HELLP syndrome. This means that as many as 48,000 women per year will develop HELLP syndrome in the United States.

HELLP syndrome can be difficult to diagnose, especially in the absence of protein in the urine and high blood pressure. Its symptoms are sometimes mistaken for gastritis, flu, acute hepatitis, gall bladder disease, or other conditions. Late diagnosis results in much higher mortality and morbidity. One of the important indicators of HELLP syndrome is *in vivo* hemolysis (disruption of red blood cells and release of hemoglobin into blood plasma). Due to the very high speed of disease progression, delays related to blood testing increase risk for the

mother and the baby. A patient's condition can severely deteriorate in just three hours, while many tests confirming diagnosis of HELLP syndrome also take several hours. Therefore, there is a need for new technologies that can confirm HELLP syndrome near patient, in minutes to address delays that can be detrimental. Here we propose and demonstrate a new technology for the detection of hemolysis, a key diagnostic symptom of HELLP syndrome. This dissertation aims to develop an important step toward early detection of hemolysis, with the goal of being able to confirm the diagnosis while there is still time to save the mother and the baby.

1.2 Research Approach

The new high-speed technology for the detection of hemolysis is based on optofludic spectroscopy. In particular, we work on absorption spectroscopy combined with microfiltration, with a focus on applications related to studies of different types of biological samples. The custom-designed and fabricated microfilters enable the effective capturing of cells that can be isolated from blood and further studied under a microscope. Absorption spectroscopy integrated on an optical fiber platform is used for material characterization. This optofluidic technology, with its miniaturized optical and microfluidic sub-systems, supports not only real-time, label-free measurements, but also allows for analysis of very small sample volumes. The combination gives high precision results, flexibility and allows for insight into the biochemistry of blood and other biological samples.

Because the specific application of this optofluidic platform is hemolysis assessment, filtering out blood cells, and measurement concentration of hemoglobin in plasma is required. The filtered cells can be next studied under a microscope in both upright and inverted configurations, since the micro-filter is a thin transparent membrane. In addition to imaging the captured cells on the microfiltering chip, this cutting-edge device provides an opportunity to

culture cells (e.g., circulating tumor cells) for further studies on the same chip. Therefore, this work provides a number of innovations: new architecture for optofluidic spectroscopy integrated on an optical fiber platform, a new method of hemolysis detection, and also a new multi-functional filter that can also serve as an imaging and culturing substrate.

1.3 Research Objectives

The objective of this dissertation is to develop a new optofluidic platform that can rapidly quantify the level of hemoglobin in blood plasma. The research requires development of a new miniature spectroscopic system, a new microfluidic system for blood filtration, and a unique integration of the microfluidic component with an optical fiber. The complete system can be applied to a number of important applications in addition to hemolysis detection.

The goal of this research is to contribute to the knowledge of science in the field of optofluidics and sensing by publishing in reputable *peer-reviewed* journals, and presenting in both national and international conferences.

1.4 Dissertation Outline

This thesis will present a new optofluidic system that combines spectroscopy with microfluidics. Some of the results were obtained in collaboration with other members of the USF Innovative Biomedical Instruments and Systems (IBIS) Laboratory.

Chapter 2 of the dissertation introduces the state of the art and describes prior research related to hemolysis detection.

Chapter 3 demonstrates the design, fabrication, and testing of a novel removable microfilter membrane that can filter cells or particles from biological samples. Additionally, there is experimental demonstration that the same removable microfilter can be used for further study of the captured cells under microscope and even for culturing.

Chapter 4 presents a new optofluidic spectroscopic device and its application towards elimination of human error in drug administration. This work has been published in the journal Sensing and Bio-Sensing Research.

In Chapter 5, further optimization of the optofluidic system for better detection of hemoglobin is addressed and then experimental detection of hemolysis demonstrated.

Chapter 6 present the application of optical sensing on a smartphone device. This platform allows developing countries or low resource areas to have a relieable, accurate, and low-cost detection tool for preeclampsia and HELLP syndrome.

Chapter 7 concludes my dissertation with an overall impact of hemolysis and the how the use of my research can reduce mortality and morbidity due to pregnancy complication. Also a short summary of future work and other clinical applications the presented platform can be addressed.

CHAPTER 2: BACKGROUND

2.1 Hemolysis

There are two types of hemolysis: *in vitro* and *in vivo*, both which negatively impacts the healthcare [3]. Additionally, millions of dollars are spent each year due to the inability to promptly detect hemolysis. World-wide *in vitro* hemolysis affects the quality of blood testing in clinical settings, including hospitals, clinics, and blood banks [4]. Furthermore, presence of *in vitro* hemolysis results in test inconsistency, and eventually, negatively influencing diagnostics and treatment.

In the case of *in vivo* hemolysis, early detection is critical for saving patient's life. This life-threating condition has devastating consequences for pregnant women suffering from hypertensive complications of pregnancies (HCP). Globally, HCP are among leading cause of maternal death, and preeclampsia is one of the most frequently observed HCP. *In vivo* hemolysis is a key symptom for one of complications of pregnancy – preeclampsia [5].

Currently, hemolysis detection in whole blood is impossible. First, blood plasma has to be separated, and then the level of hemoglobin is determined based on 'redness' of the sample via visual comparison to a color chart. While this method may have been used for a long time, it fails to effectively assess level of hemolysis at low levels of hemoglobin concentrations. It is important to note that detection of hemolysis at low level of hemoglobin is very important for a number of biomedical applications, including diagnosis and monitoring of several diseases. Furthermore, the traditional approach to hemolysis identification has other important drawbacks

besides its low accuracy. Large volumes of blood (measured in milliliters) are needed, in order to separate plasma using centrifuging method. . Though traditional analytical methods can also be used to detect hemolysis (e.g. ELISA), often reagents interfere with the measurements, which also results in inconsistency of hemolysis detection [6, 7]. Additionally, using ELISA for pre-processing of each blood sample would greatly increase cost of blood testing, and thus not feasible in developing countries and income stricken areas. Therefore, due to all these limitations of the visual assessment there is a need for an automatic method to detect hemolysis.

There are numerous benefits that the automated device can bring. First, it can really improve accuracy of *in vitro* hemolysis detection. This can help to identify unusable samples and thus improve diagnostics. It will have an important impact on healthcare and economy [3]. Second, it can help with detection of in-vivo hemolysis present in case of HELLP syndrome.

The rest of this chapter will focus on research related to hemolysis, how it affects different facets of healthcare, and how our technology can contribute to an effective detection of hemolysis.

2.2 *In-vivo* Hemolysis

2.2.1 Hemolysis and Hypertensive Disorder of Pregnancy

In-vivo hemolysis, can be linked insufficient production of red blood cells (RBCs). RBCs do not survive over their normal life span (~ 120 days). Due to certain mechanism the RBCs undertake, they are destroyed before their life span. Therefore, the body relies on the bone marrow to replenish the cells as fast as they are destroyed. Unfortunately, when the bone marrow is unable to timely replenish the cells, the patient then has low number of RBCs. This condition is known as a hemolytic anemia. Hemolytic anemia can be provoked by intravascular destruction of RBCs, which is observed for such conditions as sickle cell disease and HELLP syndrome [8,

9] [10-12]. This conditions due to hemolysis results in high morbidity in high income countries and high mortality in low income countries. In industrialized countries, number of deaths from preeclampsia and other pregnancy-related complications per number of live births is between 1 in 4000 and 1 in 10,000. However, in low income countries, this ratio is between 1 in 15 and 1 in 50 [13].

The sudden escalation of preeclampsia to eclampsia/HELLP syndrome in pregnant women, adds sufficiently to the rate of mortality. The progression from mild pre-eclampsia to severe pre-eclampsia can occur within a couple hours, without much clinical warning. Number of studies demonstrated that the level of free hemoglobin in plasma starts increasing in early pre-eclampsia, and then can reach very high level together with progression to HELLP syndrome [14, 15]. Unfortunately, the detection of *in vivo* hemolysis has increasing delays associated with testing, and often confirmed too late.

2.2.2 Clinical Diagnostics and Management of Preeclampsia/HELLP Syndrome

The diagnosis of pre-eclampsia/HELLP syndrome is made in the hospital through analysis of serial blood pressure measurements, detection of proteinuria, as well as several labs including aspartate transaminase (AST), alanine transaminase (ALT) lactate dehydrogenase (LDH), uric acid, hemoglobin/hematocrit, platelet count and a coagulation profile (PT/PTT, fibrinogen and D dimer). Patients with HELLP syndrome have a combination of elevated enzyme levels, elevated uric acid, diminished platelet count, and proteinuria. This condition is very severe, and possibly coagulopathy. The hemoglobin/hematocrit can be elevated due to hemo-concentration, or it can be reduced if the patient is coagulopathic.

When a patient has mild pre-eclampsia and is remote from term, it’s important to test periodically if the patient is deteriorating. Patients might be given magnesium sulfate as

prophylaxis of eclampsia and a course of corticosteroids to enhance fetal lung maturation. Once the diagnosis of severe pre-eclampsia and/or HELLP Syndrome is confirmed, the recommended management is the delivery of the baby. If the patient develops the associated coagulopathy, she might require transfusion of blood and/or blood products for reversal of this disorder. It is important to note that the use of corticosteroids to improve the maternal condition is controversial. Therefore, it's also important to diagnose these conditions earlier to avoid controversial approach.

2.3 *In-vitro* Hemolysis

2.3.1 Overview of *In-vitro* Hemolysis

Currently, clinicians collect, handle, and store blood specimen before sending them to laboratory. In order to ensure appropriate quality of the samples, avoiding hemolysis, there are a number of practices that has been used. It's been suggested to use straight needles venipuncture, vacuum tube, and antecubital fossa vs. more distal site [16]. Despite all this effort, sample contamination still remains a concern. This is especially true in emergency departments, which has greater than 30% rate of hemolysis [17]. Also, 60% of all rejected clinical blood specimen were rejected due to hemolysis, according to Soderberg et al [18]. Other types of sample contamination include general collection errors and serum preparation errors.

A study showed that 91% of personnel in blood testing facilities were aware of hemolysis, but only 58% of the 91% were monitoring the hemolysis level in their samples systematically and were aware of the numbers, and origin of hemolyzed samples they receive in their laboratory [19]. In a different study, of 10,709,701 samples from 453 laboratories, 37,208 samples were rejected due to hemolysis [20] and, therefore, multiple samples had to be collected from patients. For some of patients 3-5 blood samples were collected [19, 21].

2.3.2 Methods Used for *In-vitro* Hemolysis Detection

Currently, visual assessment method is used for hemolysis detection in most clinical laboratories. The color of centrifuged plasma is assessed for hemolysis either with or without reference guide, using hemolysis index (HI) [18]. The level of free hemoglobin is correlated to HI and reported as one of the following: no hemolysis, slightly hemolyzed (pink tinged), moderately hemolyzed (red), grossly hemolysis (dark red), (Figure 2.1). This method is very subjective and not standardized [22]. Different laboratories reported different detection limits for HI, i.e. HI >/= 20 or HI >/= 15, which can both represent "No hemolysis" [18, 23]. It has been showed that many hemolyzed samples assessed without reference guide were categorized incorrectly comparing to the assessment using automatic systems [4, 24]. Several automatic methods are used to assess hemolysis - ELISA and spectrophotometry methods such as Harboe method [25]. The spectroscopic methods are based on various wavelengths. Harboe method is based on near-UV spectropohotmetry, others use Soret band for a more intense signal than visible absorption band [26-28]. They all need several milliliters of blood, require plasma separation and takes time to complete, thus would not work for rapid quality assessment based on just a drop of blood.

The amount of free hemoglobin for healthy individuals is 0.001 – 0.004 g/dL (1- 4 mg/dL) [19]. For *in vivo* hemolysis which occur in pregnancy complications, total hemoglobin in whole blood of a pregnant woman is usually within the ranges from 11.6-15 g/dL (11,600 – 15,000 mg/dL) as showed in table 1. The upper limit for free hemoglobin in blood plasma of a healthy person is 0.004 g/dL (4 mg/dL). However, hemoglobin concentration that can be defined visually is greater than 30-50 g/dL [10], figure 2.1. Additionally, elevated concentration of other

blood component such as bilirubin complicates visual detection and even some analytical assays [29].

Since upper level of hemolysis in pregnancy complications can be as high as 3 g/dL and above, there is a challenge in designing a system that has a dynamic range of three orders of magnitude [19].

Table 1: Hemoglobin concentration in whole blood of women

Units	Nonpregnant Female	First Trimester	Second Trimester	Third Trimester
g/dL	12 -15.8	11.6 - 13.9	9.7 - 14.8	9.5 -15

Figure 2.1 Current visual detection method for hemolyzed samples. From left to right, ranks pure to grossly hemolyzed samples, with free hemoglobin in plasma ranging from less than 0.5 g/dL to greater than 30g/dL [16].

In summary, traditional visual assessment of hemolysis is unreliable, while available automatic measurements require extensive time and prohibitively expensive. Therefore, there is a great need in an accurate, fully automatic hemolysis assessment tool that can precisely measure free plasma hemoglobin for both *in vivo* and *in vitro* hemolysis.

2.4 Alternative Approaches to Sensing

Recent advancement in technology has improved many types of biomedical sensors. Optical detection methods such as fluorescence, absorption and Raman can be used for analysis of biomedical samples using light. Different electrochemical, optical, and thermometric methods can be used to analyze biochemistry with high sensitivity and specificity [30]. Additionally different Point-of-care testing and Lab-on-a-chip (LOC) technologies have more applications in the biological and medical fields. Below, focus is based on analyzing existing technologies and using these concept to design a new technology for hemolysis detection.

2.4.1 Spectroscopy

Optical absorption spectroscopy analyzes materials by measuring the amount of light absorbed in relation to the light frequency or wavelength. It is widely used in chemistry, biology and medicine and has high sensitivity, and specificity [30-32]. An additional benefit of spectroscopy includes real-time analysis on complex fluids without the need for preanalytical processing or large sample volumes. It is especially important for medical applications, since blood testing instruments have to be compact, operate with small blood volume (microliters), and still be precisely accurate. Furthermore, spectroscopy can be integrated with other passive and active components, such as filters, mixers, on a single microfluidic chip.

One applications of spectroscopy for biomedical applications is glucose measurement. Many researchers are trying to find a good alternative to traditional finger pricking. A semi-invasive near infrared (NIR) glucose monitoring based on absorption spectroscopy with a microfluidic chip showed detection limit of the measurements to be 20 mg/dL [33]. However, Anas *et al* demonstrated a non-invasive near-infrared glucose measurements [34]. Furthermore, since a pressing need for compressive analysis has led to demonstration of comprehensive

analysis of total biochemical composition of plasma and in blood with infrared spectroscopy was used to distinguish between cancer and non-cancer patients [35].

For application on detection of hemolysis, concentration of hemoglobin can be extracted from spectroscopic measurements using Beer-Lambert Law (1), in which absorbance is directly proportional to the path length, and concentration of an absorptive component.

$A = \mathcal{E}lc$, where A is the total absorbance, $\mathcal{E}$ is the molar absorptivity, l is the path length, and C, concentration. Alternatively, transmission T can be measured with respect to the same parameters.

$$T = \frac{I}{I_o} = e^{-\alpha l} = e^{-\varepsilon lc} \qquad \text{Equation 1}$$

where, T = Transmission of light through the system; I and I_0 are initial and transmitted light intensity.

Since different molecules absorb in different parts of the optical spectrum, this absorption "fingerprint" can be used to identify components and measure their concentration. Base on this principle, a device was designed, that can determine the concentration of hemoglobin present in blood plasma, real-time.

2.4.2 Optical Fibers

Optical spectroscopy can be conducted on large instruments, but currently there is a lot of interest in its miniaturization and integration on highly compact optical fiber platform. In general, optical fiber are great for miniature sensing because they are lightweight, have low power consumption, and high bandwidth [36], and can be used in a dangerous environment [37, 38]. Other applications of optical fibers range from networks and communications [38-41] to chemical and biomedical sensing. In particular, in sensing, optical fibers can be used to measure

temperature, pressure and other physical parameters [36], in addition to many chemical and biological substances [42].

There are many different kinds of optical fibers made from glasses and plastics and having different core/cladding configurations.

Some of them are optimized for a specific wavelength, while others support broadband signal propagation. If fiber diameter is less than 250 μm, it can be inserted into medical instruments, such as catheters, IV bags, or needles for highly localized measurements.

2.4.3 Microfluidics and Optofluidics

While optical fibers allow conducting very sensitive measurements on small samples, handling these small volumes of fluid requires use of microfluidics [43]. The integration of microfluidics with optical fibers enables creating a miniaturized platform for quantitative analysis of many biological fluids including blood, urine, and saliva [44, 45]. The field that allows this integration is called optofluidics, and it has important applications in telemedicine and point of care testing. Benefits of optofluidics include cost reduction and improved efficacy. Additionally, it can help bringing affordable, rapid and accurate medical diagnostics to lower income countries [46-48].

Currently, because of the lack of infrastructure, and low resources, many patients suffer from the lack of adequate diagnostics, which further results in lack of treatment. Improvement is needed to combat such diseases as HIV/AIDs, malaria, Ebola and many others. The 2014, United Nations report showed an increase of lives saved through malaria interventions (3 million young children between 2000 and 2012), 22 million lives saved with tuberculosis treatment, and 9.5 million people received antiretroviral medicine [49]. Though this incredible improvement has been made, almost 600 children still die every day of AIDs-related causes, and a record high

of estimated 35.3 million people still live with HIV worldwide [49]. Furthermore, 210 maternal death per 100,000 live births were recorded in 2013, this number indicate a decrease from last recording of 380 deaths, however, the report stated that much more was needed in this area to provide adequate care for pregnant women and their babies [49].

2.4.4 Mobile Medicine

Another way to conduct low cost sensing in developing countries is through the use of mobile phones. Seven billion mobile phone subscriptions were reported in the 2014 United Nation report. This means that even in a very low resource environment the mobile phones become available, and thus can be used for healthcare applications. Cell phone imaging can be seen as a grandchild of optical spectroscopy which has been used for quantitative and specific diagnosis of many disease [46]. There have been many advances in cell phone imaging and analysis [50, 51]. For example, Ozcan Lab developed a platform for mobile phone based microscopy and flow cytometry [51, 52]. Other advances of mobile phone based images include super-resolution algorithm [53, 54] allowing to conduct sample imaging with the sub-pixel resolution limits [55]. Furthermore, researchers have demonstrated mobile phone colorimetric assays. A cellphone-based urine analysis platform sensing marker PCADM-1 for prostate cancer diagnosis was developed by GENTAG, Inc and MacroArray Technologies, LLC [56]. Another system was created for *E. coli* detection. It used anti-*E.coli* antibody-functionalized arrays and a quantum dot (QD) immunoassay [57]. Additionally, this system used battery-powered ultra-violet LEDs that allowed uniform excitation of the labeled *E.coli*.

2.4.5 Point-of-Care Testing and Lab-on-a-Chip

One of important trends in contemporary healthcare is that it evolves from the standard laboratory processing using large instruments, large samples and large volumes of expensive

reagents to the use of point-of-care devices and lab-on-chip. It helps to address sanitization of device in clinical setting, improves automation and operation speed, and decreases sample volume [58, 59].

The POC and LOC platform can be applied to a number of studies in blood. For pregnant women who developed preeclampsia, the level of hemoglobin in their blood is an important indicator of the disease progression. Other important parameters of blood are uric acid, related to the kidney health, number of platelet, hematocrit, and percentage of red blood cells (RBCs) with abnormal shape and functionality. For instance, a label-free optofluidic POC device demonstrated detection of cells distribution based on size and stiffness with high sensitivity using encoded forward light scattering signal [59]. Compare to the typical blood volume needed for blood analysis, this compact, inexpensive system needed ~5 μL of human blood.

In this dissertation we integrate together spectroscopy and microfluidics on optical fiber platform and demonstrate several important POC applications of this new technology.

CHAPTER 3: A NEW APPROACH TO MICROFLUIDIC FILTRATION: MODULAR FILTERS THAT CAN BE ATTACHED AND REMOVED FROM MICROFLUIDIC CHIP

3.1 Introduction

The traditional approach to microfluidics is based on monolithic integration of multiple components on a single chip [60]. This approach allows for the simultaneous fabrication of multiple components including, but not limited to, microfluidic channels, filters, and sensors, thus enabling many functionalities [61, 62]. However, the monolithic integration of a microchip requires that all of the functional components comprising the microfluidic circuit are fixed at the time of fabrication. In order to change the parameters of the microfluidic filter or the characteristics of a sensor, the whole functional layer must be changed, new photolithographic masks must be created, and all fabrication steps must be repeated.

We propose the fabrication of some select microfluidic circuit components on separate microfluidic chips and seamlessly connecting them with the main circuit. This introduces a completely new level of flexibility to microfluidics and allows for custom integration with different kinds of sensors, filters, or other microfluidic components. In this paper, we focus on microscale filters because they are not only very important for the field of microfluidics, but frequently cause problems for the whole system operation. The ability to exchange a clogged microfluidic filter for a new one without the need to throw

away the whole microfluidic-chip would increase the economy and efficiency of future microfluidics. Furthermore, filtering on the micro-scale is needed for a broad range of applications, such as capturing circulating tumor cells, separating blood cells from plasma, and collecting high concentrations of food pathogens or other small-sized particles from complex solutions or biological samples [63-68].

3.1.1 Current Approaches to Filtering of Microparticles

Traditionally, the separation of microscale particles from a complex liquid sample requires either centrifugation [62], mechanical millilitre-scale filtering using syringes [69], vacuum filter units [70], attachable filter membranes [71], or microfluidic filtration [72-74]. Centrifugation is widely used for biomedical applications, such as the separation of blood cells from plasma. It works only on relatively large sample volumes, measured in milliliters, while many applications, (e.g., capturing circulating tumor cells) require microfiltration [75-78].

Mechanical filtration is widely used for laboratory sample pre-processing; tissue culture; biological fluids; fixation buffers; particle removal and clarification. This strategy is most effective for work on large scales or for high volumes and pressures [79-81]. The filtering membranes used for this approach can be made from a variety of materials, such as regenerated cellulose, polyethersulfone, surfactant-free cellulose acetate, nylon, or "PTFE" fluourocarbon resin. Yet this is not an effective approach for work that requires small volumes or for on-chip applications [82].

Processing of small fluid samples requires the use of microfluidics. One approach is to use size-restrictive filtration based on micro-pillars and micro-channels [83-86]. However, fluid flow through these structures requires high pressure and frequently results in

damage to the filters or degradation of biological samples [77] through induced blood hemolysis and cell fragmentation.

3.1.2 Sample Processing After Microfiltration

While there are multiple microfluidic filters [65-68, 75-77], their main purpose is typically limited to filtering out unneeded particles or cells. However, it is frequently necessary for on-chip micro-filtration to be followed by microscopic or spectroscopic analysis of captured microscale objects, or by fluorescence in situ hybridization (FISH) [78, 88, 89]. Previously, this analysis has been completed after filtration using specialized instruments [90-92]. The inconvenience and cost of the aforementioned approach has created a need to simplify the extraction of captured objects before conducting analysis. This can be done using removable building blocks for microfluidics that can be easily inserted or extracted from the microfluidic circuit.

3.1.3 Experimental Approach

Here we demonstrate a new, modular, microfluidic filter that can be attached to a microfluidic chip and later removed or exchanged for another filter. The filter is a thin porous transparent membrane with a pore size smaller than the particles being filtered [93]. It can easily be attached to microfluidic chips to capture particles; then be detached and used for particle analysis under a microscope or for spectroscopic studies [94]. Using a 1μm thick membrane instead of long microfluidic channels helps to significantly increase filtering area, decrease the pressure, and eliminate damage to the biological samples. Furthermore, if the accumulation of a large number of particles prevents microfluidic flow, the filter can be easily removed and exchanged for a new one. This modular configuration provides a simple, convenient tool for fast isolation and analysis of

cells, bacteria, and micro-particles. Additionally, this new technology can be used fora broad range of chemical, biomedical and safety applications.

3.2 Materials and Methods

3.2.1 Membrane Fabrication

The modular microfluidic filter captures particles using a porous membrane with a periodic array of holes shown in (Figure 3.1a). It was fabricated using the process flow shown in (Figure 3.2a-f). In order to enable the separation of a variety of particles from solution, numerous designs consisting of different pore sizes and configurations were fabricated on a single photolithographic mask. The pore sizes ranged from 1µm to 20µm in diameter, and each device was contained inside of a 5 mm square.

The detailed fabrication procedure used for processing was the following (Figure 3.2). To begin, 1µm thick layers of silicon nitride were deposited on double-side polished wafers using the Nitride Tystar low pressure chemical vapour deposition (LPCVD) diffusion furnace at GATech MiRC facility; details of the LPCVD preparation process can be found here [89]. Next, photolithography was conducted using a chromium mask and AZ4620 photoresist; followed by silicon nitride etching in a PlasmaTherm reactive ion etcher and the removal of the residual photoresist. The backside of the same wafer was then photo lithographically patterned after careful alignment of the front and back structures [95].

The next process step was silicon etching of the wafers in a heated solution of potassium hydroxide [94]. After this was completed, the micro-filtering membrane was released from the underlying silicon and a small chamber with a height equal to thickness of the wafer was formed. The backside of the chamber was patterned with a large circular

opening. The scanning electron microscope (SEM) image of the completed device is shown in (Figure 3.1). The small chamber together with the top and bottom membrane is shown in the image.

When fabrication was completed the devices were cleaned and diced using a dicing saw. After this, the hydrophilic properties of the membrane were tested to make sure that the fluid would run through the pores without the need to apply high pressure. Figure 3.3 shows that the contact angle for the water of water drop on the membrane was 35.7° and that the membrane was hydrophilic.

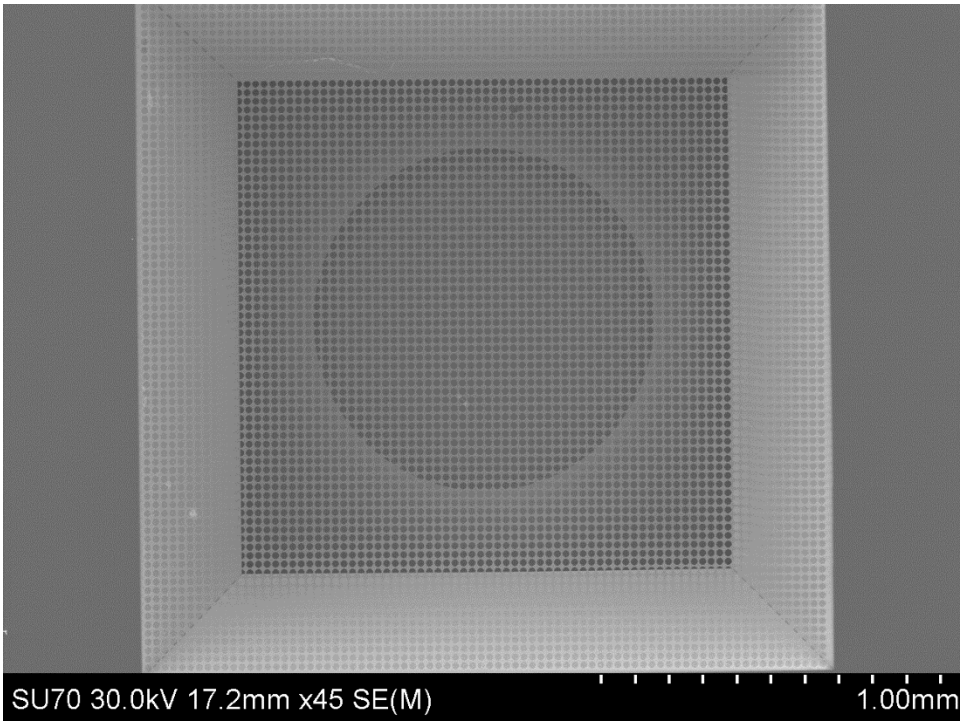

Figure 3.1 SEM image of a micro-fabricated filtering membrane. The large square is the membrane on top side of the wafer. It has a periodic array of holes through which we can see a smaller square which is a membrane on the bottom side of the wafer that has one circular hole in the middle.

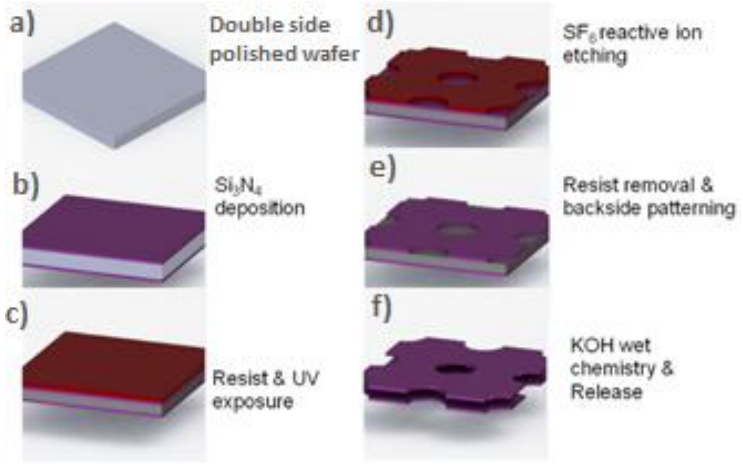

Figure 3.2 Fabrication process for the transparent reconfigurable microstrainer. (a, b) Low stress silicon nitride is deposited on both sides of a double side polished wafer. (c, d) Photoresist is spin-coated; photolithography is used to pattern pores in the membrane followed by the etching through the nitride layer. (e) The wafer is flipped and the backside is patterned using photolithography and etching. (f) To complete the fabrication, KOH is used to release the structure.

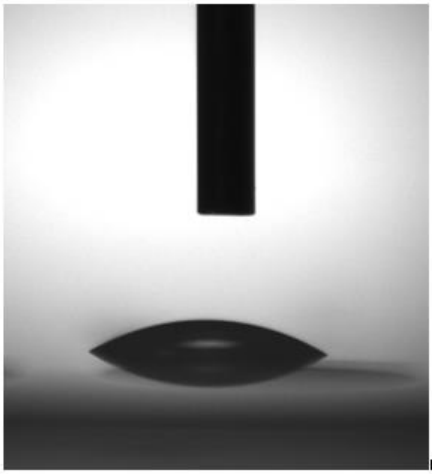

Figure 3.3 Water contact angle measured on the surface of the fabricated membrane

3.2.2 Packaging and Integration

Here we propose two approaches towards packaging of the modular membrane. The integration of the filtering membrane into a microfluidic device requires the membrane to be encapsulated across micro-channels containing the solution to be filtered. The first approach is shown in Figure 3.4; in this method, the filtering membrane is still attached to the supporting piece of silicon substrate and is sandwiched between two

Polydimethylsiloxane (PDMS) adapters inserted between two glass slides (Figure 3.4 a-d); The purpose of the PDMS adapters is to hold the membrane in place by touching only the supporting substrate, but not the membrane. Even though the membrane is very robust (after integration into the microfluidic system it can operate continuously for hours without breaking), the direct attachment to the membrane is challenging because it is very thin. The PDMS structure protects the membrane which allows for simple assembly and disassembly of the filter. Along with the adapters, glass slides are used to provide mechanical support and to facilitate integration with capillary tubes. To achieve this, a small opening is drilled into two glass slides in which thin capillary tubes are inserted. The complete device can then be connected to other microfluidic chips through these tubes. Figure 3.4 e-f demonstrates how this microfluidic filter would separate red blood cells from a blood sample and provide blood plasma as the filtrate. This application would be very beneficial for many diagnostic microfluidic chips that work well with blood plasma, but fail with whole blood.

Figure 3.5-a shows a variety of membranes with differing sizes and pore diameters all fabricated on a single 3-inch wafer. After the wafer is diced, an individual chip, with a selected membrane size, is inserted into the configuration described in Figure 3.4. Figure 3.5 b shows the complete assembly that includes a membrane with 6μm pores Figure 3.5 c. Figure 3.5 d) and e) show the second approach towards filter device assembly, where the micro-channels and the insertion chamber are moulded in PDMS. This second strategy simplifies the insertion and removal of the filtering membrane, yet, this comes with the cost of a slightly more difficult tubing attachment when compared to the first integration approach. Both methods work equally well, and the choice of one over the

other depends on the specific application of the filter and the consideration of future integration with the design of other microfluidic chips.

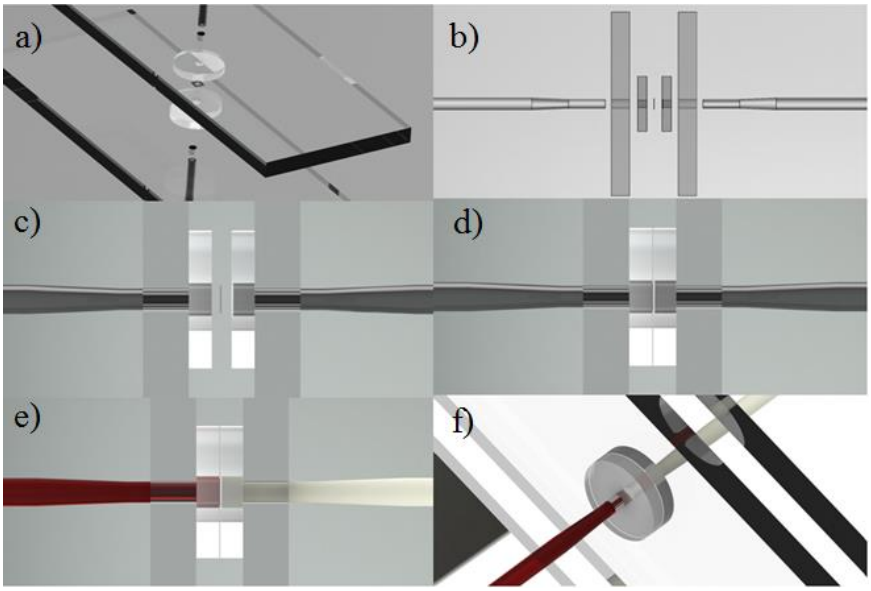

Figure 3.4 3-Dimensional model of proposed integration of the filtering membrane into a microfluidic filter. The membrane is sandwiched between two protective PDMS adapters inserted between two glass slides (a-d). The proposed filtering of the whole blood sample is shown in (e-f).

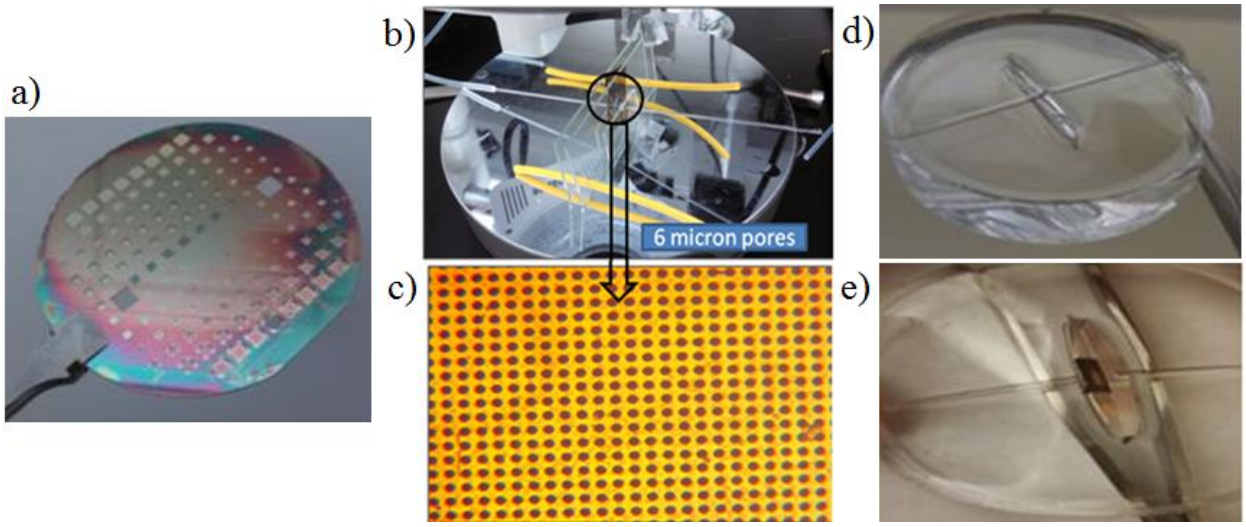

Figure 3.5 Integration of the membrane into a microfluidic filter. (a) A 3-inch silicon wafer with multiple microfabricated filtering membranes. (b) Membrane sandwiched between supporting glass slides with the tubes attached. (c) Close-up of the integrated membrane that has a periodic array of pores each one 6 μm in diameter. (d) and (e) show an alternative approach to integration, where the whole microfluidic structure including microfluidic channels is moulded in PDMS. The membrane is inserted across the channels.

3.3 Results and Discussions

3.3.1 Microfluidic Filtration and Further Sample Processing

The microfluidic filter was tested with a variety of solutions (Figure 3.5) and it was demonstrated that the membrane can effectively separate particles from the filtrate. (Figure 3.5a) shows the filtration of a solution that consisted of a high concentration of dark brown microspheres in water. The brown fluid flows from the left, and after going through the membrane that is inserted perpendicular to the microfluidic channel, the fluid becomes clear (on the right). The fluid was pumped using peristaltic pump with a minimum flow rate of ~2μL/s working at the lowest setting. Microchannels were moulded in PDMS using very thin capillary tubes. The microfiltering membrane was inserted perpendicular to the channel for filtration and later extracted for analysis of the captured particles. Figure 3.6 b demonstrates that cells can be successfully captured using the same microfilter with a pore diameter smaller than the cells being used. The cells in this experiment are Human Lung Fibroblasts, IRM-90, from ATCC.

The filtering ability of the membrane depends on the size of the pores along with the size of the particles; when large particles are captured, smaller ones can still go through. (Figures 3.6 c and d) demonstrate 20 μm microbeads captured on a membrane with 10 μm pores. Figure 3.6 c is focused on microbeads, while Figure 3.6 d is focused on the membrane. Figures 3.6 e and f show that the particles that are smaller than the membrane pores can easily flow through the pores to the other side of the membrane. By focusing above and below the transparent membrane, particles can be observed on both sides. It is also demonstrated that focusing through the membrane produces an image of

almost identical quality when compared with directly observing the particles on top of the membrane.

3.3.2 Filtration Operation

The design configuration of the circular opening (figure 3.1) enables the extraction of fluid medium from particles and cells. Yet, the filtration of particles of different sizes requires tight control of the change in pressure across the membrane to keep the larger particles from damaging the thin transparent silicon nitride membrane. To achieve this control is it necessary to know the volumetric flow rate, Q. Given in equation 1 below, Q is calculated knowing the diameter of the capillary *D*, the velocity of the fluid *V*, and the viscosity of the fluid, γ, (for distilled water it is $0.894 \times 10^{-3}\ Pa.s.$).

$$Q = \frac{\pi}{4} D^2 V \qquad \text{Equation 1}$$

The volumetric flow rate is related to the pressure across the membrane by the Hagen Poiseuille equation.

$$\Delta P = \frac{8\gamma L Q}{\pi r^4} = \frac{128\gamma L Q}{\pi D^4} \qquad \text{Equation 2}$$

where viscosity, γ and volumetric flow rate, Q are used along with channel length, L and channel diameter D.

It was observed that efficient particle separation, without damage to the membrane, was achieved when the V was measured as $1.79 \times 10^{-3}\ m/s$. Based on this velocity, Q was calculated to be $2\ \mu L/s$ and the pressure drop across the membrane while particles are filtered (Figure 3.6) was calculated as $2.70 Pa$.

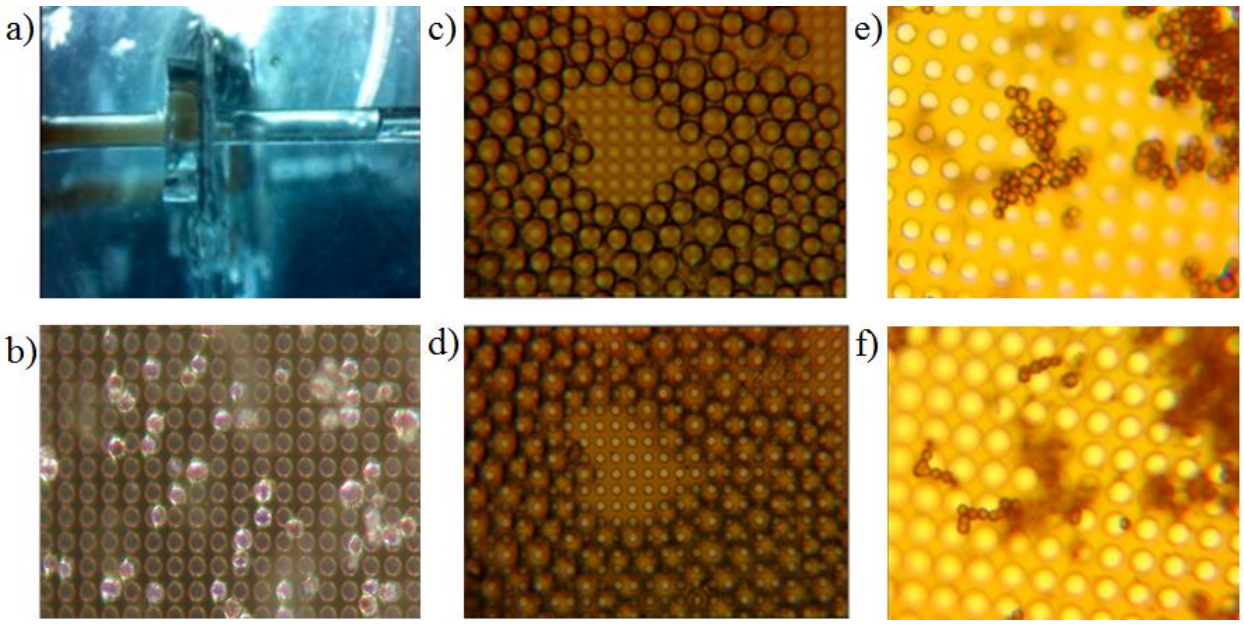

Figure 3.6 Demonstration of microfluidic filtration. (a) Filtration of concentrated particle solution. (b) Filtered Human Lung Fibroblasts cells. (c) and (d) show 20 µm microbeads captured on a membrane with 10 µm pores with a focus on beads (c) and the membrane (d). (e and f) are focused above and below the transparent membrane and show that small particles can go through the membrane.

3.3.3 Biological Sample Integrity

In the next experiment, captured Human Lung Fibroblast cells were cultured directly on the microfiltering membrane in 10% FBS/1% antibiotic medium Figure 3.7. Figure 3.7a demonstrates that the cells were successfully attached to the membrane and were able to grow. Figure 3.7b shows fluorescent image obtained using a LIVE/DEAD® Cell Viability Assay. In this figure the cells fluoresce with green light demonstrating that they are all alive.

For safety, all experiments with captured or cultured cells on the microfiltering membranes were completed in an aseptic environment. The membranes were cleaned with ethanol solution (70%); removing all chemical residues. Next, fibronectin was coated on the membrane to assist in the cell adhesion and mitosis. For culturing, the

membrane was used without any further preparation steps; however for fluorescent imaging, cells were incubated in a 1:1 fresh medium mixed with fluorescence dyes.

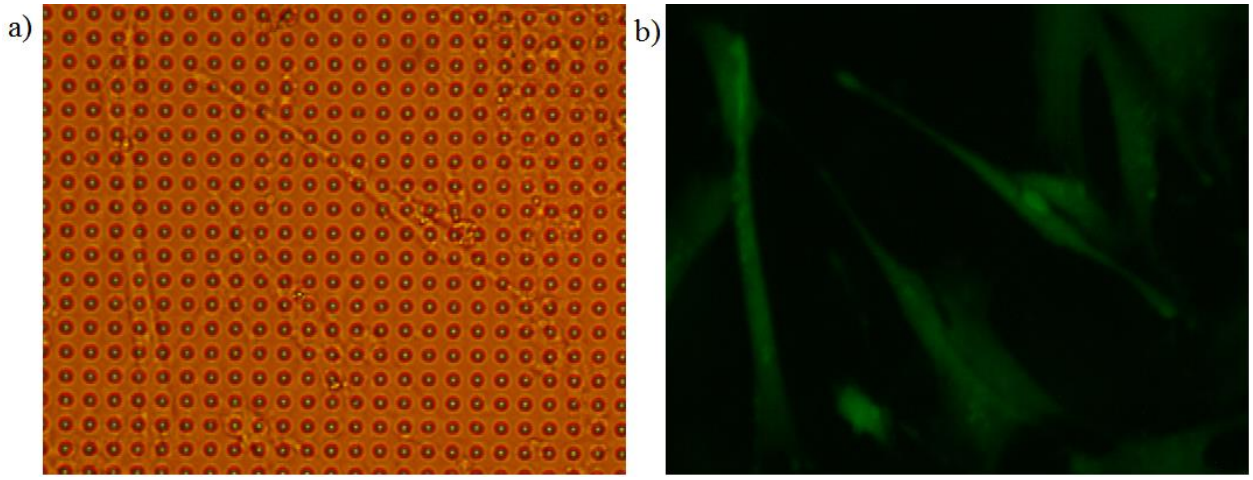

Figure 3.7 Microfiltering membrane with the Human Lung Fibroblasts cells grown on its surface. (a) Optical microscopy image of the membrane with the cells. (b) Green fluorescent images of cells demonstrating that all of them are alive.

3.4 Conclusion

We have designed, fabricated, and tested innovative modular microfluidic filters that can be used as an exchangeable building block for the implementation of complex microfluidic circuits. Filtering and capturing of particles and cells from a number of fluids has been demonstrated; along with the ability to use the same filter for the analysis of the captured content. The thin transparent microfiltering membrane can be used for bright field and fluorescent microscopy and even for the culturing of captured cells. This device has a multitude of potential applications in microfluidics ranging from the capturing and analysis of the circulating tumor cells, to other industrial applications including food analysis, safety and security.

CHAPTER 4: OPTOFLUIDIC SPECTROSCOPY INTEGRATED ON OPTICAL FIBER PLATFORM[1]

4.1 Introduction

The Institute of Medicine estimated that as many as 98,000 patients die each year due to preventable medical errors, making this the sixth leading cause of death in the United States, and claiming more lives than diabetes or Alzheimer disease [96]. Additionally, the expense of medical care necessitated because of medical errors, lost income, and disability, results in a total cost between $17 billion and $29 billion per year [97]. There are many potential sources of error in patient care, such as medical prescriptions, transcriptions, dispensing and administration of drugs, and monitoring patient's responses. However, among these, administration errors account for approximately 32% of morbidity and mortality cases in inpatient facilities [97]. Because of this, there is a pressing need to detect drug identity and concentration during administration, allowing for precise measurement of dosages, and preventing errors in real time before adverse effects take place.

While monitoring of specific medications such as antidepressants and anticoagulants are important for compliance and toxicity checks [98], there are many other pharmaceuticals that when wrongly administered will result in dangerous consequences [99]. Currently, several specialized assay based techniques have been used to monitor medication errors in specific therapeutic treatments, known as therapeutic drug monitoring (TDM) [98-101]. However, assay and label based detection systems such as immunoassays, electrochemical assays, and lateral-

[1] This chapter was previously published. Permission is included in Appendix A.

flow assays (LFAs) have several limitations that prevent them from being used for point-of-care sensing [102]. These techniques are time consuming, and require large volumes of analyte to achieve the needed sensitivity. Furthermore, drug assays use complicated electrochemical measurements, suffer from background interference in complex solutions and have poor thermal stability [103-109]. Currently there are no available technologies for detection of overdose or incorrect drugs during administration.

There are many sensors that can work in almost real time and do not require use of reagents, but they typically measure refractive index and are based on ring-resonators [110-113], photonic-crystals [114-116], whispering gallery-mode [117-119], plasmonic structures [120] and other optical components, that without additional modifications do not provide enough specificity for differentiation between multiple drugs. In addition, these techniques are prone to noise caused by any microscale particles present in the system and are very sensitive to small temperature changes.

In general, traditional approaches to drug identification include color test [121], microscopic microcrystal analysis [122], thin layer chromatography [123], gas chromatography [124], mass spectroscopy [125], X-ray diffraction [126], and different types of spectroscopy that are most suitable for real time detection. By using traditional spectroscopic techniques (IR, Near-IR, NMR, Raman) it has been shown that drug identity can be determined [127-130]. Once a drug has been identified using traditional spectroscopy, information regarding concentration may be obtained by quantifying absorption at a specific wavelength. Furthermore, spectroscopy using a single optical fiber is becoming a powerful approach for analysis of biological samples [131-135].

However, for complex systems such as biological fluids that contain a variety of free floating particles and cells, the effectiveness in determining a drugs concentration is significantly reduced due to scattering and interference by these objects. As a result, additional reagents are required to amplify the spectral signatures of compounds of interest (e.g. biomarkers of a specific multiple diseases) [136-138]. Unfortunately, studies requiring reagents and labeling can only be performed in specialized laboratories, using large sample volumes, as well as extensive time for analysis ranging from several hours to multiple days. Because of this, a reliable, reagent and label-free, detection method that can run in real-time by using a small sample volume would greatly benefit point-of care drug monitoring.

To overcome these limitations we have proposed a new optofluidic platform that can be used to detect the concentration of drugs by absorption spectroscopy, free of noise from particles and cells, without prior sample pre-processing. This device is small enough that it can be directly inserted to an IV bag or syringe, and continuously monitor drug concentration before or while the patient is being treated. Additionally, this device can be mass-produced and requires relatively inexpensive materials.

4.2 Materials and Methods

4.2.1 Device Principles

The device was designed to be a compact probe, consisting of a miniature microfluidic chamber attached to the interface of an optical fiber (Figure 4.1). The bottom of the microfluidic chamber consists of a porous membrane that allows fluids and chemical compounds to flow inside the device, while at the same time filtering out undesired particles. Furthermore, the porous membrane is coated with a reflective metal. Because of this coating, light will pass through the filtered fluid and reflect back once it reaches the membrane. The reflected light can

then be collected by the optical fiber for spectroscopic analysis of the filtered fluid. Based on the absorption of light by the fluid, the system can provide a conclusion if the drug dosage is correct. The top portion of the chamber might also contain small pores to allow air to escape while the chamber is being filled. Alternatively, if the top portion of the chamber is not inserted in fluid, then it might have larger air outlets.

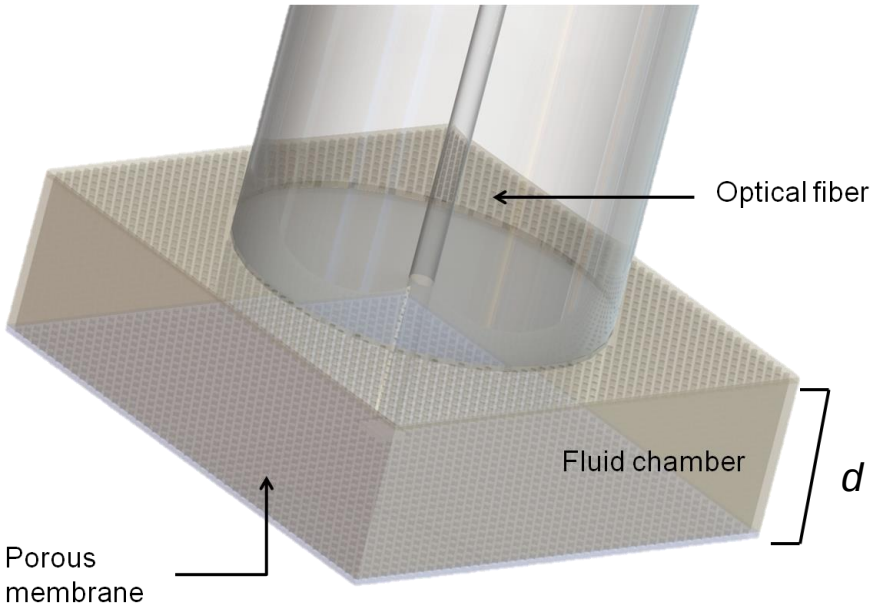

Figure 4.1 Artistic rendering of the design of the optofluidic probe and its main components. This includes optical fiber with attached microfluidic chamber. Sample fluid would propagate through the micrometer-size pores while particles are filtered out. The bottom membrane is reflective, so light exiting the fiber into sample fluid contained in the chamber is coupled back into the same fiber for analysis.

4.2.2 Fabrication Flow

The reflective micro-porous membrane for the fluid chamber was fabricated using standard micro-fabrication processes (Figure 4.2) [139, 140]. Double-side polished silicon wafers purchased from Nova Electronic Materials (Texas) were used as the substrate (Figure 4.2 a). First, a 1 µm thick membrane layer of silicon nitride (Si_3N_4) was grown on both sides of the wafer by low stress–low pressure chemical vapor deposition (LPCVD) at the MiRC facility at Georgia Tech (Figure 4.2 b). Wafers were cleaned with acetone and IPA, then dried with

nitrogen. Additionally, they were baked on hotplate @ 115ºC for 5 minutes to dehydrate and then cooled for a couple of minutes before spin-coating with photoresist.

Next, Si_3N_4 layer was patterned (Figure 4.2 c), defining the transparent microfiltering membrane on one side and optic fiber opening on the other side. It was done by spin-coating positive photoresist followed by UV lithography and reactive ion etching on both sides of the wafer. Two consecutive photolithography steps required through-wafer alignment using IR mask aligner. The recipe for the photoresist deposition was the following: 4620AZ Positive Resist was spin-coated first at 4000rpm for 30 seconds, then at 500rpm for 10 seconds and finally at 6500rpm for 60 seconds. This allowed to achieve the most uniform surface coverage. Then it was baked in oven at 100°C for 20 minutes and rehydrated for 24 hours. The exposure was 7 seconds on Karl Suss mask aligner (lamp intensity 25 mW/cm^2). After that it was developed for 3 min in photoresist 400K developer, hard baked at 100°C for 30 minutes and used for etching in RIE.

After patterning silicon nitride layers the exposed silicon was etched away in a solution of potassium hydroxide (KOH, 85°C) for 7 hours, creating a hollow chamber between the two nitride layers. This chamber will be filled with the fluid under study through the nitride membrane. Finally, 200 nm of gold was deposited on top of the nitride membrane using a Denton Thermal Evaporator. An optical microscopy image of the micro-fabricated membrane is shown in Figure 4.2 f. The circular pores of the membrane are 10 μm in diameter, and have been patterned in a square array with the distance of 15 μm from center to center. This configuration of the membrane allows for filtration of particles larger than 10 μm in diameter.

4.2.3 Filtration Experiment

Once the membranes had been prepared, their filtration capabilities were tested. The membranes were pre-wetted and cleaned by flushing them with acetone while switching from sample to sample. The membranes were positioned underneath an upright optical microscope for observation, where the membrane surfaces were oriented perpendicular to the microscope objective. They were slightly elevated, allowing for space to exist beneath them. In order to observe filtration with these membranes, a droplet of DI water containing naturally occurring contaminants (dust) was placed on top of the membrane surface. By relying on gravitational forces alone, the droplet of water was allowed to pass through the membrane, while contaminants were effectively filtered out. These effects were recorded using a microscope camera. After the filtration experiment was completed, the membranes were easily cleaned by rinsing with acetone.

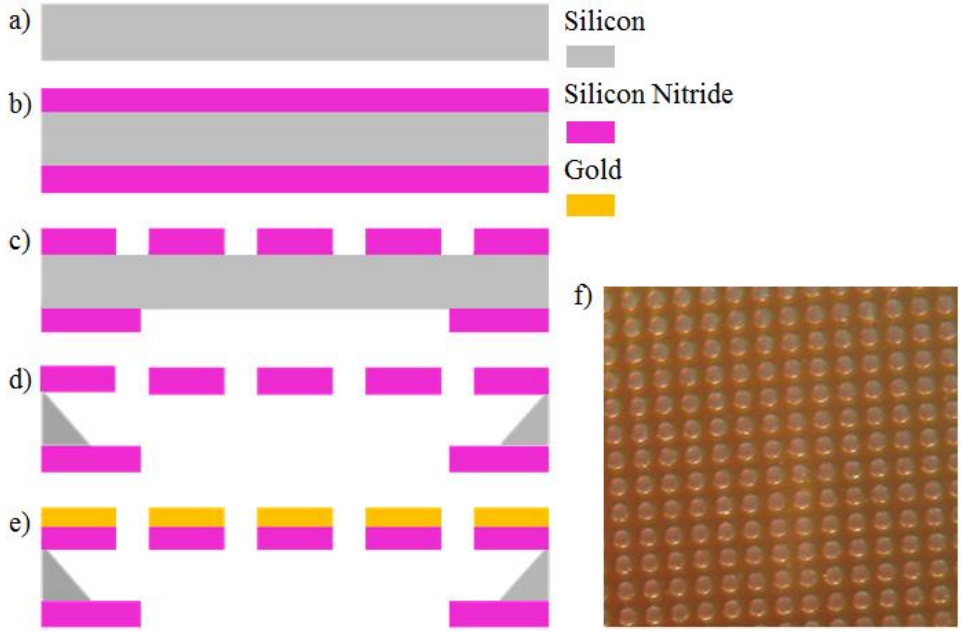

Figure 4.2 Device fabrication. (a) Two-side polished silicon substrate. (b) Silicon nitride is deposited on both sides of the wafer. (c) Silicon nitride was patterned and etched on both sides. (d) The membrane was released using etching in KOH solution. (e) Gold was deposited on the membrane. (f) Optical microscopy image of a released membrane.

4.2.4 Optical Experiments

4.2.4.1 Device Packaging

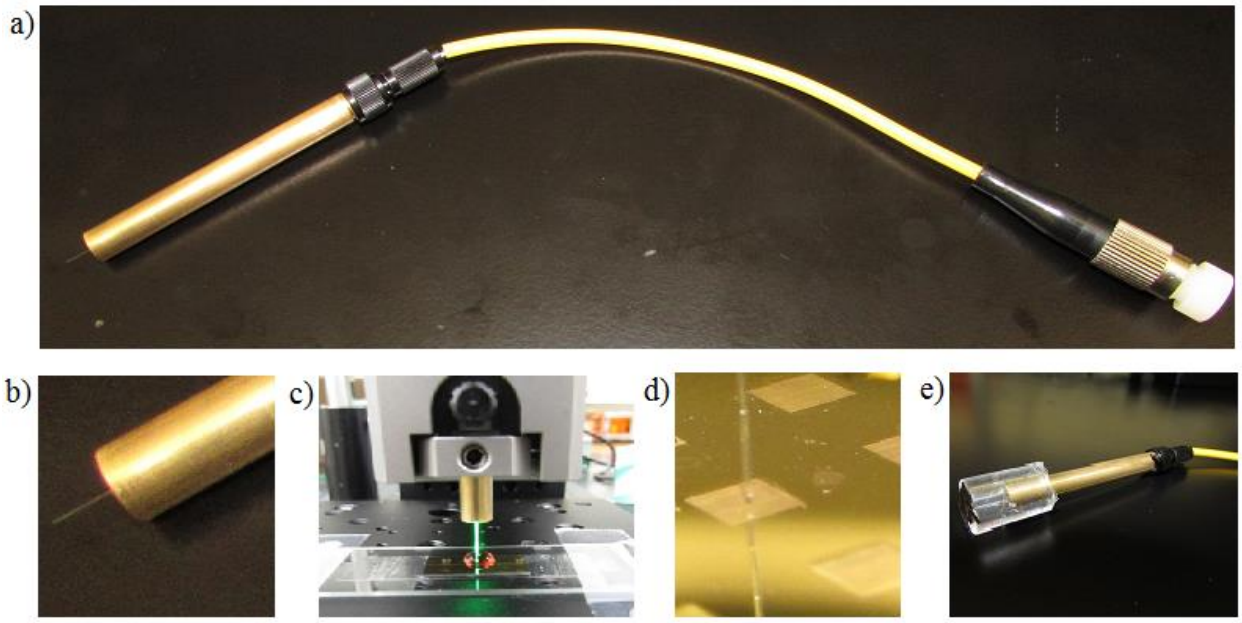

Figure 4.3 Details of the packaging. a) Cleaved optical fiber inserted into fiber holder, b) enlarged tip of the fiber that is 125 µm in diameter. c) Optical fiber holder fixed in high precision XYZ-stage. d) Optical fiber above reflective gold coated membrane. e) Fully assembled device with an optical fiber enclosed inside of the fluid chamber and a filtering membrane connected at the bottom.

After testing filtering properties of the micro-filtering membranes they were assembled next to the optical fiber tips. For this, an 8 µm optical fiber was cleaved and inserted into an adjustable fiber holder (Figure 4.3a) to provide mechanical support to the otherwise flexible fiber. The enlarged image of the exposed fiber tip is shown in Figure 4.3b. Following this, the fiber holder was inserted into a high precision XYZ-stage, and the tip was positioned ~105 µm from a reflective metal membrane by adjusting the dial of the optical stage (Figure 4.3c). For optical alignment procedures, please refer to the following section (2.4.2). In Figure 4.3d, an enlarged image of the fiber tip and membrane in the assembly is shown. It may be seen that spacing (~105 µm) exists between the fiber and the membrane, and that the membrane itself is

coated with gold. Finally, the entire device was fixed in place by epoxying the metal surrounding the membranes to a small polydimethylsiloxane (PDMS) tube. This tube was created to fit tightly to the optical fiber holder, and the final assembly can be seen in Figure 4.3e.

4.2.4.2 Fiber Alignment and Positioning

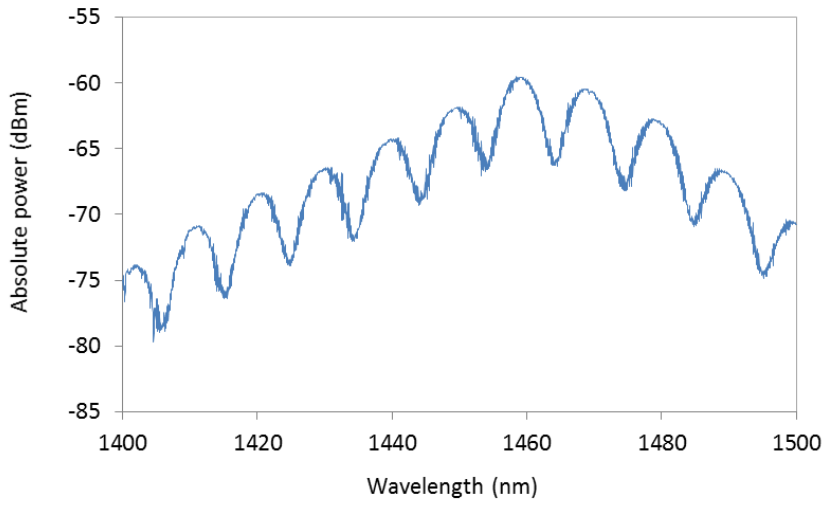

Figure 4.4 Fabry-Perot resonance of the set-up used in this experiment. Here the resonance corresponds to a separation of approximately 105 μm between the fiber and reflector.

As previously stated, before the setup was fixed in place the optical fiber and membrane required alignment and positioning at an appropriate spacing. In order to optimize coupling, the optical fiber was set perpendicular to the membrane. Angular alignment of the system was performed by adjusting the XYZ-stage, and observing the reflected power in air. An approximation of fiber angle was made qualitatively through visual observation. However, for added precision, reflected power was recorded while the fiber angle was finely tuned. The fiber angle was set once the reflected power reach a maximum value.

Following angular alignment, the fiber needed to be placed at a set spacing from the membrane surface. The XYZ-stage allows for vertical adjustment of the fiber. However, micron level precision was needed to effectively determine the spacing, and thus Fabry-Perot resonance

was used for high precision measurements. The resonance was formed between the two reflective surfaces - the gold coated membrane and the cleaved fiber interface. The spectrum was recorded in air (refractive index: 1.0) and conducted using infrared light between 1400 and 1500 nm (shown in Figure 4.4 for the desired spacing). Using the collected IR spectrum, the distance could be calculated using the following expression:

$$d = \frac{{\lambda_i}^2}{2n(\lambda_{i+1} - \lambda_i)} \qquad \text{Equation 1}$$

where λ_i and λ_{i+1} are consecutive resonance wavelengths (nm), n is the refractive index. By recording resonance patterns for different vertical settings of the XYZ-stage, a correlation between stage setting and the actual distance, determined by equation 1, was obtained. Once the appropriate vertical setting was found, the fiber was fixed in position and the distance was verified again using Fabry-Perot resonance. In Figure 4.4, we can see the Fabry-Perot resonance recorded for the vertical setting once the fiber was set 105 μm from the membrane.

4.2.4.3 Absorption Spectroscopy of Cobalamin

In order to demonstrate that the device is capable of determining drug and its concentrations, absorption spectroscopy was conducted for a specific pharmaceutical– cobalamin (vitamin B_{12}). Different drugs can be identified using UV-vis spectroscopy. For example, absorption spectrum of cobalamin dissolved in water with concentration 60 mg/dL is shown in Figure 4.5a. When drug is known, its concentration can be measured at one specific wavelength, since it is much faster than measurements of the whole spectrum.

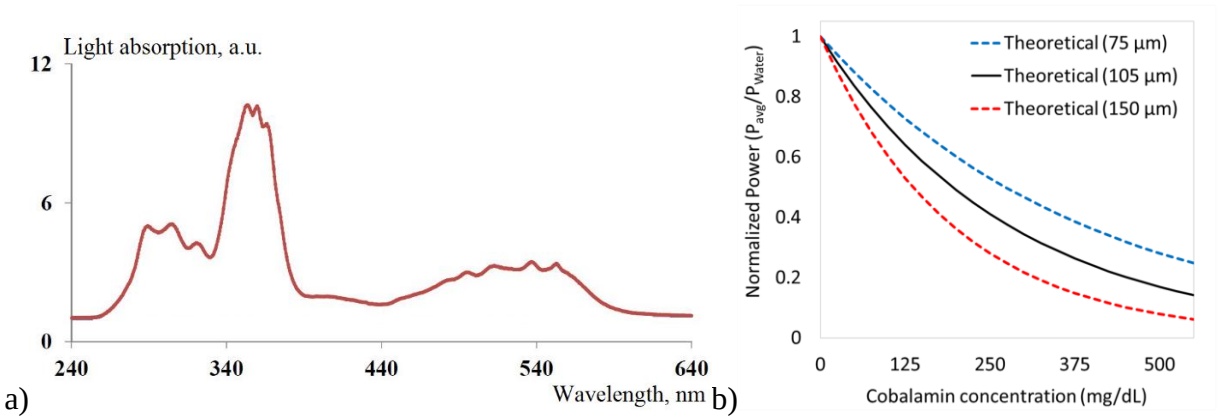

Figure 4.5 Experimental absorption spectrum. (a) and theoretical transmission profiles for Cobalamin (b) at varying concentrations and fiber spacing.

The goal was to construct a sensor that would be able to conduct measurements for the broad range of concentrations from 0.1 mg/dL to 500 mg/dL. Theoretical modeling of this sensors transfer function was conducted using Beer-Lambert law:

$$\frac{P}{P_o} = exp(-2\alpha dC) \qquad \text{Equation 2}$$

where P is the power of transmitted light (W) for the fluid under study, Po is the transmitted power (W) for a pure sample, α is the molar absorptivity with units of L/mol·cm, 2·d is the total optical path where d was the spacing between the fiber and reflective surface (cm), and C is the concentration of the cobalamin expressed in mol/L.

Figure 4.5 shows the theoretical transfer functions plotted for the needed range of concentrations and three different spacing between the fiber and the membrane – 75, 105 and 150 µm. While 150 µm gap is better for the measurements of lower concentrations, and 75 µm works better for higher concentrations, the 105 µm gap is suitable for both ranges and thus was chosen for the experimental testing.

During the experiment, the concentration of cobalamin was varied from approximately 0.1 mg/dLto 515 mg/dL, while reflected power was recorded for each concentration. All

measurements were conducted over 5 minute timeframes, during which the power was averaged. A high stability green laser (532 nm) was used at a fixed power at 30 mW. After one cobalamin measurement was made, the sample was removed, and the sensor was thoroughly rinsed with water. This cleaning was conducted to prevent build-up of cobalamin on surfaces. After cleaning, the setup was allowed to air dry for approximately one minute, ensuring that all water was removed from the system. Samples were tested sequentially with increasing concentration. In order to ensure reproducibility of results, every test was calibrated with respect to the water control measurements.

4.3 Results and Discussion

4.3.1 Filtration Demonstration

As previously mentioned, the filtering properties of the micro-fabricated porous membrane were demonstrated with a drop of DI water. Figure 4.6a and 4.6b show the empty membrane placed horizontally under the microscope and a membrane right after putting a drop of water, respectively. It may be noticed that the water passes through the pores in the membrane, and forms a drop on the other side, while all particles are filtered by the pores and remain on the membrane surface (Figure 4.6b-f). Figure 4.6f demonstrates the outline of the water drop that is not fully seen since it is already under the membrane, and the dark spots are particles that are present in all real world samples and were successfully filtered out by the membrane.

For cleaning purposes the membrane was flushed with acetone. It was observed that this also improved its wetting properties. While without applying additional pressure, water flow takes several minutes to completely pass through the membrane. However, prior prewashing decreases this time to seconds (Figure 4.6 g-i). The membrane was also tested continuously with

the lowest setting of a peristaltic pump pumping fluid with the flow rate ~2µL/s, and it could withstand the external pressure still demonstrating successful particle filtration.

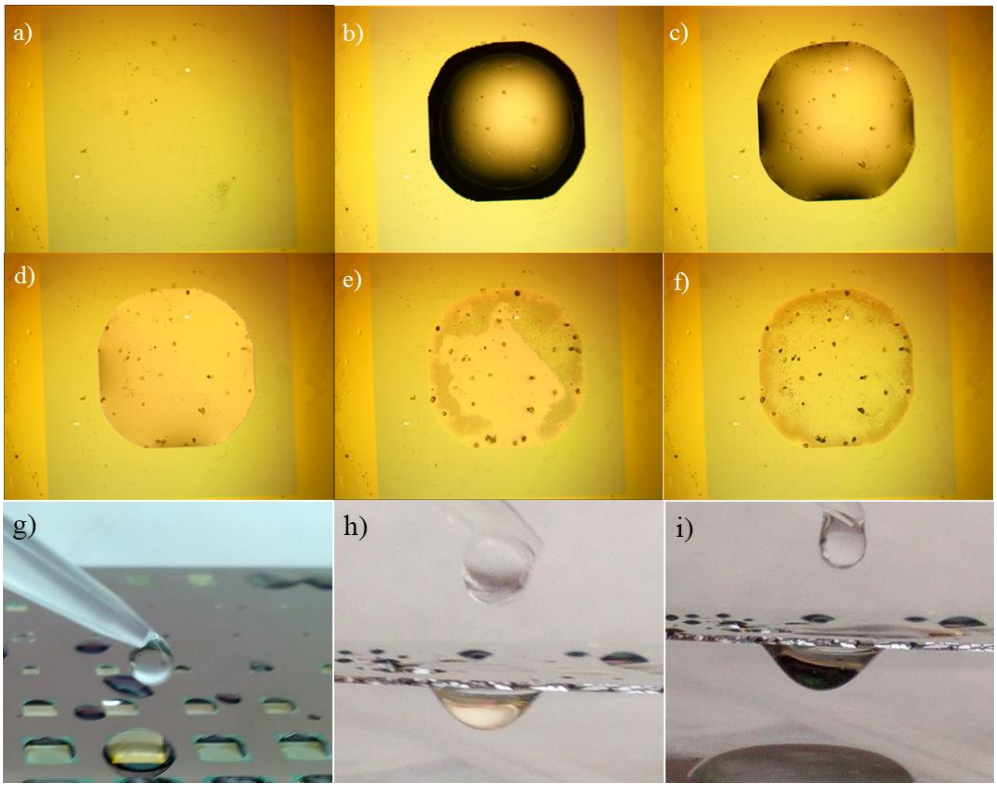

Figure 4.6 Demonstration of successful filtration using microfluidic membrane. While water goes through the membrane for further analysis, all the contamination stays on the surface.

4.3.2 Optical Measurement of Cobalamin Concentrations

While the proposed optofluidic platform is compatible with a broad range of drugs, here we demonstrated measurements of cobalamin concentration as an example drug that can be monitored using this approach. Cobalamin (vitamin B_{12}) is an essential water-soluble vitamin, of which a deficiency can lead to abnormal neurologic and psychiatric symptoms. This may include ataxia (shaky movements and unsteady gait), muscle weakness, spasticity, incontinence, hypotension (low blood pressure), vision problems, dementia, psychoses, and mood disturbances. There is a variety of doses that are used for injections: from 0.2µg/kg for neonates and infants to 1000 µg total for adults with severe vitamin deficiency [141]. This means range of

concentrations from 1 µg/ml to 1000 µg/ml, therefore the Figure 4.7b shows measurements of concentrations between 1 µg /mL to 5 mg/mL to monitor the physiological range and potential overdose.

Because cobalamin was the only compound sensed, all the measurements were conducted with a single wavelength, 532 nm, where cobalamin has high absorption and the sensor would have the highest sensitivity. In future sensing at multiple wavelengths can be used to monitor mixture of several drugs simultaneously.

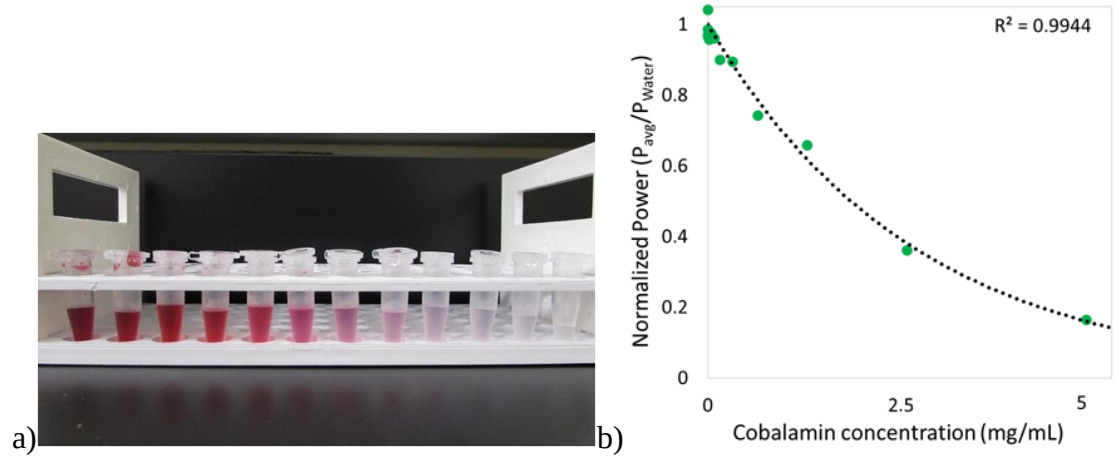

Figure 4.7 Sample of cobalamin concentrations and experimental results. a) Samples of different concentrations of cobalamin arranged in order of decreasing concentration. b) Corresponding experimental results of optical measurements of cobalamin concentration.

Figure 4.7 (a) shows the solutions of cobalamin used in this experiment in order of decreasing concentration (left to right). As a results, the experimental points are well fitted by the theoretical curve obtained using Beer-Lambert Law (R^2=0.994).

4.4 Conclusion

In conclusion, we presented a new optofluidic platform for near-patient drug monitoring designed with the purpose of providing additional level of safety for drug administration and decreased human error. This has the potential of reducing preventable deaths due to medical

errors. By combining spectroscopic analysis with microfluidic filtration, the system allows rapid and accurate testing for drug concentrations levels. Design, optimization, fabrication and experimental testing of this system for the measurement of cobalamin concentration demonstrated that this approach is promising. Furthermore, it opens up a whole area of optofluidic fiber based drug monitoring where future work includes analysis of multiple drugs and their mixtures and integration with syringes and IV-bags.

CHAPTER 5: DESIGN OF AN OPTOFLUIDIC SENSOR FOR RAPID DETECTION OF HEMOLYSIS

5.1 Introduction

Every day millions of blood samples are collected in hospitals and clinics for analysis, and a significant portion of those samples are compromised due to hemolysis: up to 31% for blood drawn in emergency rooms and 10% in blood banks and blood testing facilities [19, 142]. Significant effort has been devoted to reducing the rate of hemolysis in blood samples by optimizing collection techniques, through the use of appropriate needles and other methods; however, no significant improvement has been demonstrated [4]. Additionally, there are many causes of later hemolysis of a correctly collected blood sample, such as improper sample collection, handling, transportation, and storage [4, 24] .

This high rate of blood sample compromise negatively influences several aspects of the healthcare system and has a pronounced adverse economic impact. Millions of dollars are wasted each year because instruments for prompt, low-cost hemolysis detection are not available. Diagnoses are delayed, and some tests produce erroneous results, evidence to the fact that hemolysis is the leading cause of pre-analytical errors [24, 143]. Hemolysis interference also affects a number of important biochemical tests, such as lactate dehydrogenase (LD), aspartate aminotransferase (AST), bilirubin, cholesterol, and glucose tests. The quality of blood test results can be compromised even when the level of hemolysis is undetectable by visual inspection (plasma hemoglobin less than 50 mg/dL) [144]. In addition to sample contamination

due to *in vitro* hemolysis, *in vivo* hemolysis is also a problem, resulting in vascular disease, inflammation, thrombosis, and renal impairment [7]. Evidence of hemolysis can be detected at 10 mg/dL in some conditions, while grossly hemolyzed samples might have free plasma hemoglobin concentration of 500 mg/dL and above.

Currently there is no reliable way to detect hemolysis without first separating the blood plasma from the whole blood sample. The traditional detection method is visual assessment of the level of "redness" of the separated plasma. This approach, however, results in a high percentage of human errors and miscategorizations. Alternatively, there are several automatic methods of free plasma hemoglobin measurement such as ELISA and spectrophotometry [145] [25-27]. These automatic methods of hemolysis detection are time-consuming and expensive. As a result, these methods do not work well for rapid assessments of sample quality.

Here we propose a new device that allows for quantitative measurement of the level of hemolysis of just a drop of plasma using absorption spectroscopy. Quantitative measurements are available instantaneously, and the method is reagent-free. Significantly, this portable device can be used for quality control in blood testing facilities or in hospitals before blood transfusions. For the above reasons, we optimized the instrument for the range of measurements between 0 and 500 mg/dL.

5.2 Device Packaging and Design

Detection of hemolysis requires that measurements be made of free plasma hemoglobin. It cannot be done in whole blood samples because of interference from unlysed blood cells. Thus, the cells must first be separated from the sample before the plasma can be analyzed. This can be achieved by centrifugation and then using an optical fiber platform and absorption spectroscopy techniques to measure hemoglobin concentration. Figure 5.1a shows the proposed

design, while Figure 5.1b shows the assembled prototype. Here the whole structure is inserted into a molded PDMS tube with a thin capillay. A cleaved optical fiber can be fixed in a fiber holder that can be moved freely within filtered plasma. The PDMS forms an airtight seal with the fiber capillary holding the fiber holder and fiber.

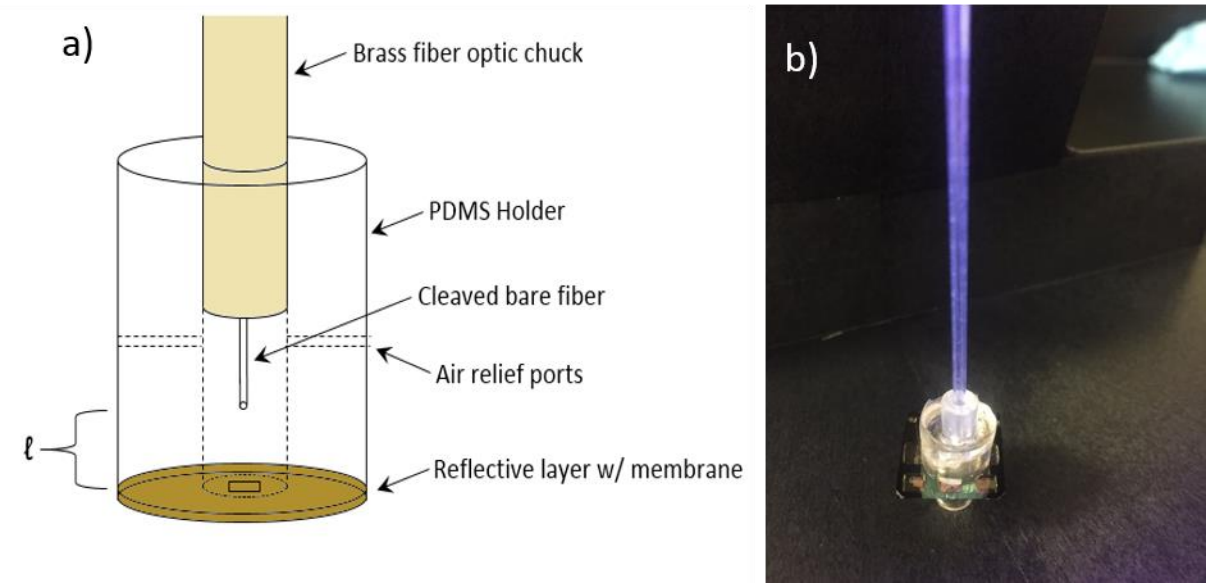

Figure 5.1 Proposed design for the spectroscopic probe. a) Proposed design for the spectroscopic probe. b) Fully assembled spectroscopic probe, including optical fiber, PDMS holder, and reflective membrane.

A thin (~1 μm) reflective porous membrane is attached at the bottom of the chamber. The reflective membrane is fabricated using a conventional photolithographic process with gold deposition, as described in a previous work [28]. Specifically, silicon nitride was deposited on a double-side silicon wafer, and positive resist was used for design patterning. After photolithography, nitride etching and wet-etching for silicon layer, 200 nm of gold was deposited on the silicon nitride membrane. The supporting wafer was attached using epoxy to ensure a watertight seal. Pores (1–3 μm in diameter) were etched across the whole membrane in a square array. The entire device, fully assembled for experimental use, is shown in Figure5.1b.

A drop of plasma can be applied on the surface of the membrane that, through capillary action, moves into the miniature chamber and inserted capillary. The plasma can subsequently be analyzed. Spectroscopic analysis of plasma is performed to measure the concentration of free hemoglobin. Light from the optical fiber passes through the fluid, eventually reaching the reflective gold coated membrane. The reflected light is couple back to the optical fiber into the power meter for measurement. The whole device can be inserted into acetone for a quick flush, as an easy cleaning technique.

5.3 Optimization of Optical Parameters

Hemolysis is detected by measuring the concentration of hemoglobin in the plasma. Light absorption is measured with a single optical fiber (Figure 5.1a), and then the Beer-Lambert law is applied. The Beer-Lambert equation relates light transmission to the concentration of optically absorptive compounds in a sample.:

$$T_\ell = \exp(-2\alpha\ell C) \qquad \text{Equation 1}$$

where ℓ is the spacing distance between the tip of the optical fiber and the reflective membrane (cm), C is the concentration of hemoglobin in the plasma (mol/L), α is the wavelength-dependent molar absorptivity of hemoglobin (L/mol·cm), and T_ℓ is the resulting fraction of light transmitted through the sample at the set spacing ℓ.

Hemoglobin is found naturally in two variations (oxygenated and deoxygenated), which must be taken into consideration. Both variations of hemoglobin have own distinct values of molar absorptivity (α) at different parts of the electromagnetic spectrum. However, for a few wavelengths of light (isosbestic points), α for oxygenated and deoxygenated hemoglobin is the same. Over the wavelength range from 500 to 600 nm, four isosbestic points occur, at approximately 530, 545, 570, and 584 nm, with α values of 0.0138, 0.0188, 0.0167 and 0.0127

L/mol·cm, respectively [94]. The advantage of using isobestic points is that a single wavelength can be used to determine the total (both forms) concentration of hemoglobin. For this method, a wavelength of 545 nm was selected because of the high corresponding absorption.

After choosing the wavelength (thus determining the molar absorptivity), there remain three unknown variables of the Beer-Lambert equation ($eq.$ 1). Hemoglobin concentration (C) is the variable we wish to determine, and transmission (T_ℓ) is the variable we can directly measure. The spacing (ℓ) can be chosen such that the sensor operates with an optimum level of performance.

Figure 5.2 shows the influence of the spacing (ℓ) on the transfer function relating light transmission to hemoglobin concentration. Fiber spacing is chosen depending on the desired range of sensor measurements. For example, if expected hemoglobin concentrations can be up to only 100 mg/dL, then a larger fiber spacing (4.0 mm) would be chosen to achieve the best resolution within that range. It will allow to accumulate larger optical absorption in thicker layer of plasma and extract more information about low hemoglobin concentrations. If much higher concentrations of hemoglobin are to be measured, then a smaller spacing should be chosen.

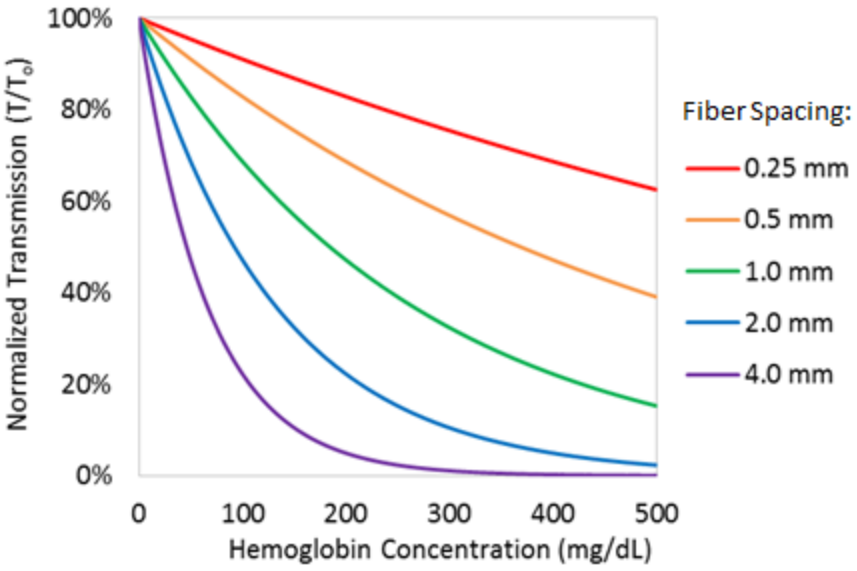

Figure 5.2 Transfer functions relating normalized for different spacings (ℓ) between the fiber and the reflective membrane.

For a sensor that displays exponential decay as its operating curve, we consider performance to light transmission to hemoglobin concentration, be optimal when there exists a strong negative decay over the concentration range of interest. This allows for distinct and well-defined changes in transmission, as well as greater sensitivity in resolving concentration values. However, the performance curve must not display too steep of an exponential decay, as the sensor would then lose sensitivity in resolving concentrations at the extremities of the range of interest.

To characterize sensor behaviors over a range of hemoglobin concentrations, two operation parameters were created through manipulations of statistical curve regression analysis and least squares error. These parameters are the fraction of maximum decay (ψ) and the degree of curvature (φ). The fraction of maximum decay is a measure of how much the signal 'decays' over the range of interest (C_a to C_b). A value of zero indicates a curve with no decay, while a value of one implies that maximum decay has been reached over the range of interest (i.e., transmission at C_b is 0%). Derivation and simplification of this parameter is shown in *eq. 2*.

$$\psi = \left(\frac{T_\ell(C_b) - T_\ell(C_a)}{C_b - C_a}\right)\left(\frac{C_b - C_a}{T_\infty(C_b) - T_\infty(C_a)}\right) = 1 - \frac{T_\ell(C_b)}{100\%} \qquad \text{Equation 2}$$

In Equation 2, transmission T_ℓ is written as a function of concentration *C*, and the denotation ℓ signifies that the separation between the fiber and membrane is at a fixed length ℓ. As such, T_∞ is the transmission that corresponds to a fixed separation for which the tip of the optical fiber and the reflective membrane are infinitely far apart. The other parameter, the degree of curvature φ, measures the extent to which the exponential sensor deviates from a linear operation behavior. A degree of curvature near one indicates that the curve is behaving approximately linear, and as this value decreases, the operation curve deviates from a liniar fit over the range of interest. This parameter was derived through modification of the least squares correlation coefficient, to describe the squared error between the exponential operation curve 'T_ℓ' and a hypothetical performance curve for a linear sensor 'θ_ℓ.' Expressions for φ and θ_ℓ are given below in Equation 3 and 4 respectively.

$$\phi = 1 - \frac{\int_{C_a}^{C_b}(\theta_\ell - T_\ell)^2 dC}{\int_{C_a}^{C_b}(\theta_\infty - T_\infty)^2 dC} = 1 - \frac{\int_{C_a}^{C_b}(\theta_\ell - T_\ell)^2 dC}{\int_{C_a}^{C_b}(\theta_\infty)^2 dC} \qquad \text{Equation 3}$$

$$\theta_\ell = \left(\frac{T_\ell(C_b) - T_\ell(C_a)}{C_b - C_a}\right) \cdot C + 100\% \qquad \text{Equation 4}$$

Solving Equation 1 through 4 for an effective hemoglobin concentration range from 0 to 500 mg/dL and iterating over various spacings (ℓ), the two behavior parameters could be calculated (Figure 5.3a). When the spacing is near 0 mm (i.e., fiber and membrane are nearly touching), the sensor behaves practically linearly; however the rate of decay is significantly low. Conversely, at larger separation lengths, the decay rapidly reaches its maximum value; however, the sensor operates exponentially. By multiplying the two parameters (φψ), the optimum

behavior can be determined by locating the relative maximum value, which in turn reveals the optimal spacing required to achieve this desired behavior. Figure 5.3b shows the results of this multiplication, with a maximum value at approximately 1.27 mm.

Figure 5.4 shows the theoretical transfer function for the proposed hemolysis sensor based on solving the Beer-Lambert law (*eq*. 1) for the optimal spacing. Knowing the optimum chamber length, this operating curve for the sensor can be achieved. This indicate that transmission drop between a pure plasma (0 mg/dL of hemoglobin) to a slightly hemolyzed sample of (30 mg/dL) is approximately 13% change.

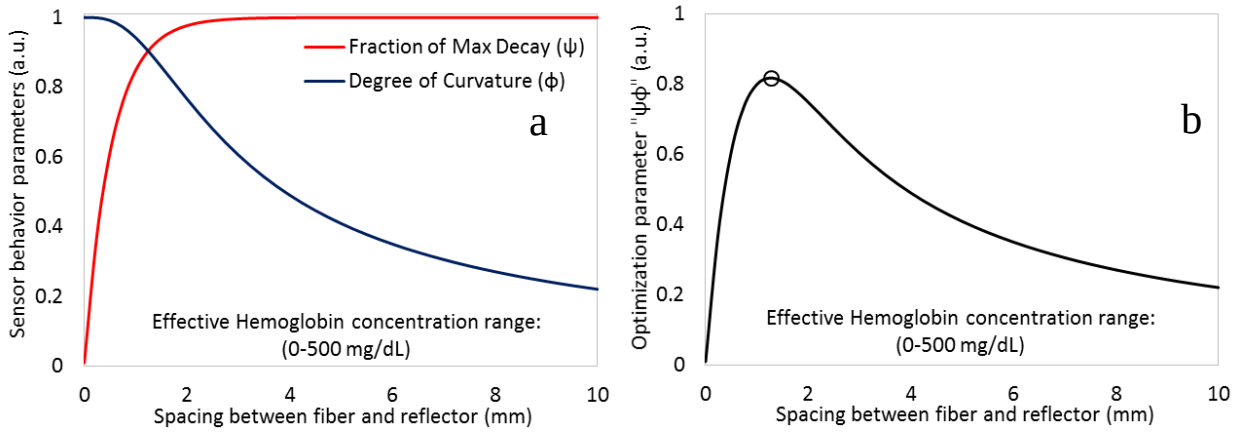

Figure 5.3 Sensor parameter optimization based on optical detection of hemoglobin over the concentration range 0–500 mg/dL. a) Parameters describing sensor behavior are shown for various chamber lengths, ℓ. b) Multiplying these two parameters, a spacing for optimum optical performance can be found.

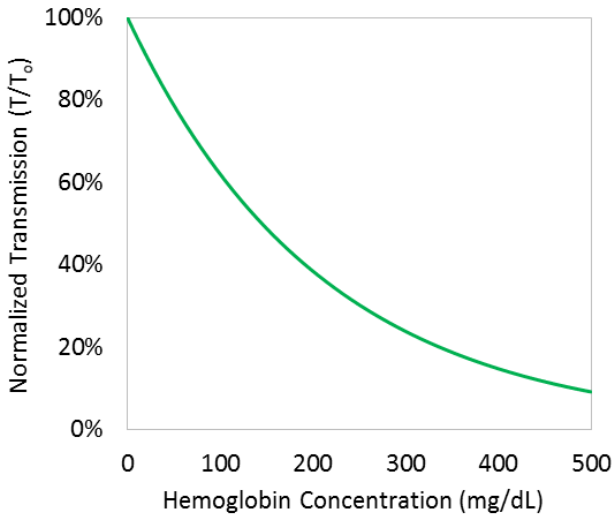

Figure 5.4 Theoretical performance curve for the optimum sensor configuration over normalized transmission measurement of wide range of hemoglobin concentration measured in milligrams per deciliter (mg/dL).

5.4 Experimental Detection of Hemoglobin

Measuring the distance between the gold-coated membrane and the optical fiber is crucial for determining the exact concentration of hemoglobin in a plasma sample. Therefore, a 200 µm cleaved optical fiber was inserted into a fiber holder, which was then connected to an XYZ-stage and adjusted to a distance of about 1025 µm from the gold surface. The system was optically aligned by adjusting the XYZ-stage and observing the reflected power when the chamber was filled with either air or water. The recorded Fabry-Perot resonance formed between the cleaved fiber and the gold surface was used to determine the precise distance and to adjust it to the needed value [146]. Figure 5.5 shows theoretical and experimental analysis of the percentage of light lost due to diffraction for different optical fibers. It can be noticed that for the propagation lengths we are interested in, optical fiber with 200 µm core diameter loses the lowest amount of light.

Serial concentration solutions of hemoglobin were then prepared in blood plasma using animal plasma and hemoglobin from bovine blood lyophilized powder. The reflection

measurements were taken over a large range of concentrations (0–500 mg/dL). Each set of measurements was repeated three times over duration of 5 minutes for each concentration of hemoglobin. All the measurements were normalized relative to the initial laser power. The results can be seen in Figure 5.6, a plot of the averaged power vs. hemoglobin concentration.

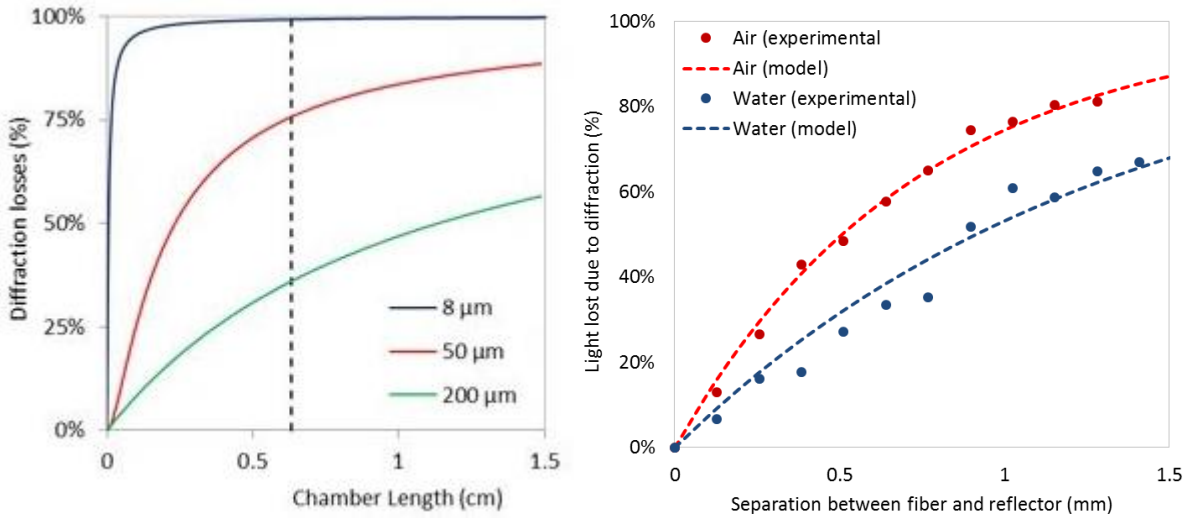

Figure 5.5 Left: Percentage of light lost due to diffraction for 8, 50 and 200 µm core optical fiber. Right: Losses were measured for the chamber filled either with air (red) or water (blue), and model curves were fit to the experimental data.

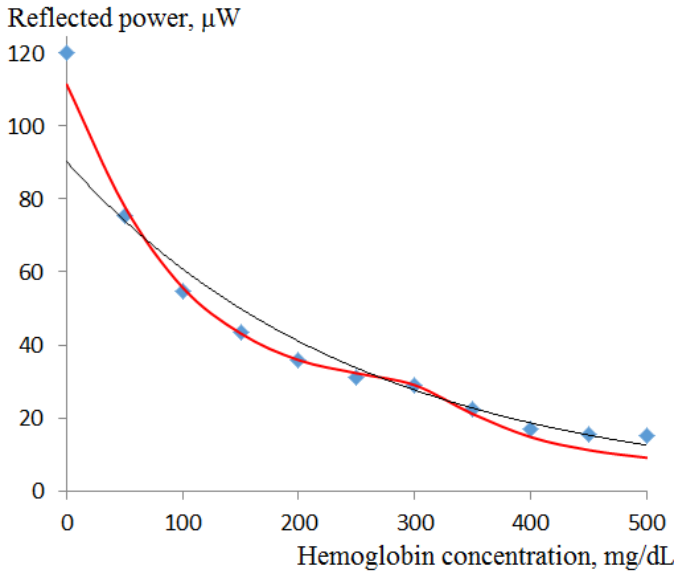

Figure 5.6 Experimental results showing decrease of reflected light with increase of hemoglobin concentration. The data points show exponential decay due to increased absorption together with periodic fluctuations because of the change of refractive index in the Fabry-Perot resonator.

5.5 Conclusions

A method for rapidly detecting hemolysis, using only microliters of plasma, has many critical applications for blood-testing quality control and safety control. In this work, we proposed, theoretically optimized, fabricated, and tested miniature instrument to rapid test for hemolysis in plasma samples for a broad range of hemoglobin concentrations. This sensing platform integrates the optical fiber technology and the microfluidic reflective membrane.

CHAPTER 6: CONCLUSIONS AND FUTURE WORK

The negative impact of hemolysis has significantly affected healthcare as well as national and global economy. To address these worldwide health concerns, we specifically focused on hemolysis in maternal complications. A novel biomedical platform, optofluidic device was investigated for point-of-care clinical and analytical assessment of hemolysis for implementation in low resource settings and the developing world. A combinatory approach was taken by integrating optics and microfluidics. As a result, a new device was introduced with successful fabrication of the 3-dimentional microfilter. The proposed microfilter would enable a new direction in the field of microfluidics analysis. This system will be useful not only toward this research, but in any microfiltering system, where spectroscopic analysis is needed real-time. The developed platform can be applied for affordable, rapid and accurate testing in other areas such as protein level quantification, and diseases such as sickle-cell.

In addition to the microfilters, a mobile platform was designed to accurately quantify hemolysis by assessing the levels of hemoglobin through color analysis. Results of this work showed successful detection of critical levels of hemoglobin due to hemolysis without any sample pre-processing. This achievement was to target preeclampsia and HELLP syndrome rapidly, near-patient, especially in developing countries. An international patent was filed during this project and clinical assessments will be continued toward improving the device and mobile platform.

REFERENCES

1. Organization, W.H., *Make every mother and child count.* World Health Report 2005, 2005(Geneva: WHO).

2. *Preeclampsia and Maternal Mortality: a Global Burden.*

3. Ong, M.E.H., Y.H. Chan, and C.S. Lim, *Reducing blood sample hemolysis at a tertiary hospital emergency department.* The American journal of medicine, 2009. **122**(11): p. 1054. e1-1054. e6.

4. Stauss, M., et al., *Hemolysis of coagulation specimens: a comparative study of intravenous draw methods.* Journal of Emergency Nursing, 2012. **38**(1): p. 15-21.

5. Hansson, S.R., Å. Nääv, and L. Erlandsson, *Oxidative stress in preeclampsia and the role of free fetal hemoglobin.* Frontiers in Physiology, 2014. **5**: p. 516.

6. Jay, D.W. and D. Provasek, *Characterization and mathematical correction of hemolysis interference in selected Hitachi 717 assays.* Clinical chemistry, 1993. **39**(9): p. 1804-1810.

7. Koseoglu, M., et al., *Effects of hemolysis interference on routine biochemistry parameters.* Biochemia medica, 2011. **21**(1): p. 79-85.

8. Dhaliwal, G., P.A. Cornett, and L.M. Tierney Jr, *Hemolytic anemia.* Am Fam Physician, 2004. **69**(11): p. 2599-2606.

9. Tabbara, I., *Hemolytic anemias. Diagnosis and management.* The Medical clinics of North America, 1992. **76**(3): p. 649-668.

10. Bessler, M., A. Schaefer, and P. Keller, *Paroxysmal nocturnal hemoglobinuria: insights from recent advances in molecular biology.* Transfusion medicine reviews, 2001. **15**(4): p. 255-267.

11. Gehrs, B.C. and R.C. Friedberg, *Autoimmune hemolytic anemia.* American journal of hematology, 2002. **69**(4): p. 258-271.

12. Packman, C.H., *Hemolytic anemia due to warm autoantibodies.* Blood reviews, 2008. **22**(1): p. 17-31.

13. Duley, L., *Pre-eclampsia and the hypertensive disorders of pregnancy.* British Medical Bulletin, 2003. **67**(1): p. 161-176.

14. Sandrim, V.C., et al., *Increased circulating cell-free hemoglobin levels reduce nitric oxide bioavailability in preeclampsia.* Free Radical Biology and Medicine, 2010. **49**(3): p. 493-500.

15. Rother, R.P., et al., *The clinical sequelae of intravascular hemolysis and extracellular plasma hemoglobin: a novel mechanism of human disease.* JAMA, 2005. **293**(13): p. 1653-62.

16. Giuseppe Lippi, G.C., Emmanuel J. Favaloro, Mario Plebani, *Hemolysis: An unresolved dispute in laboratory medicine.* 2002. **4**.

17. Heyer, N.J., et al., *Effectiveness of practices to reduce blood sample hemolysis in EDs: a laboratory medicine best practices systematic review and meta-analysis.* Clinical biochemistry, 2012. **45**(13): p. 1012-1032.

18. Söderberg, J., et al., *Haemolysis index–an estimate of preanalytical quality in primary health care.* Clinical Chemistry and Laboratory Medicine, 2009. **47**(8): p. 940-944.

19. Giuseppe Lippi, G.C., Emmanuel J. Favaloro, Mario Plebani, *Hemolysis, An Unresolved Dispute in Laboratory Medicine*, in *In Vitro and In Vivo Hemolysis*. 2012.

20. B.A. Jones, R.R. Calam & P.J. Howanitz, Arch Pathology laboratory Medicine, 1997,121, 19-26

21. Heyer, N.J., et al., *Effectiveness of practices to reduce blood sample hemolysis in EDs: A laboratory medicine best practices systematic review and meta-analysis.* Clinical Biochemistry, 2012. **45**(13–14): p. 1012-1032.

22. Šimundić, A.-M., et al., *Hemolysis detection and management of hemolyzed specimens.* Biochemia medica: časopis hrvatskoga društva medicinskih biokemičara, 2010. **20**(2): p. 154-159.

23. *Interference Indices.* Cornell University College of Veterinary Medicine ECLINPATH.

24. Lippi, G., et al., *Special issue: Quality in laboratory diagnostics: from theory to practice.* Biochemia Medica, 2010. **20**(2): p. 126-30.

25. Adamzik, M., et al., *Free hemoglobin concentration in severe sepsis: methods of measurement and prediction of outcome.* Critical Care, 2012. **16**(4): p. R125.

26. Harboe, M., *A Method for Determination of Hemoglobin in Plasma by Near-Ultraviolet Spectrophotometry.* Scandinavian Journal of Clinical & Laboratory Investigation, 1959. **11**(1): p. 66-70.

27. Fairbanks, V., S. Ziesmer, and P. O'Brien, *Methods for measuring plasma hemoglobin in micromolar concentration compared.* Clinical chemistry, 1992. **38**(1): p. 132-140.

28. Noe, D.A., V. Weedn, and W.R. Bell, *Direct spectrophotometry of serum hemoglobin: an Allen correction compared with a three-wavelength polychromatic analysis.* Clinical chemistry, 1984. **30**(5): p. 627-630.

29. Lippi, G., et al., *Preanalytical quality improvement: in quality we trust.* Clinical chemistry and laboratory medicine, 2013. **51**(1): p. 229-241.

30. Dey, D. and T. Goswami, *Optical biosensors: a revolution towards quantum nanoscale electronics device fabrication.* J Biomed Biotechnol, 2011. **2011**: p. 348218.

31. Vo-Dinh, T. and P. Kasili, *Fiber-optic nanosensors for single-cell monitoring.* Anal Bioanal Chem, 2005. **382**(4): p. 918-25.

32. Fang, Y.L., et al., *Optical properties and photocatalytic activities of spherical ZnO and flower-like ZnO structures synthesized by facile hydrothermal method.* Journal of Alloys and Compounds, 2013. **575**: p. 359-363.

33. Ben Mohammadi, L., et al., *In vivo evaluation of a chip based near infrared sensor for continuous glucose monitoring.* Biosensors and Bioelectronics, 2014. **53**(0): p. 99-104.

34. Anas, M.N., et al. *Non-invasive blood glucose measurement Application of near infrared optical measurement*. in *Sustainable Utilization and Development in Engineering and Technology (STUDENT), 2012 IEEE Conference on*. 2012.

35. Zelig, U., et al., *Early detection of breast cancer using total biochemical analysis of peripheral blood components: a preliminary study.* BMC cancer, 2015. **15**(1): p. 408.

36. Francis, T., S. Yin, and P.B. Ruffin, *Fiber optic sensors*. 2010: CRC press.

37. Mckenzie, J.S. and C. Clark, *High sensitivity micromachined optical-to-fluid pressure converter for use in an optical actuation scheme.* Journal of Micromechanics and Microengineering, 1992. **2**(4): p. 245.

38. Jones, B.E., *Optical fibre sensors and systems for industry.* Journal of Physics E: Scientific Instruments, 1985. **18**(9): p. 770.

39. Mynbaev, D.K. and L.L. Scheiner, *Fiber-optic communications technology*. 2001: Prentice Hall New York.

40. Liu, A., et al., *High-speed optical modulation based on carrier depletion in a silicon waveguide.* Opt. Express, 2007. **15**(2): p. 660-668.

41. Hecht, J. and L. Long, *Understanding fiber optics*. Vol. 3. 2002: Prentice Hall Upper Saddle River, NJ.

42. Cheng, S.-F. and L.-K. Chau, *Colloidal gold-modified optical fiber for chemical and biochemical sensing.* Analytical chemistry, 2003. **75**(1): p. 16-21.

43. Testa, G., G. Persichetti, and R. Bernini, *Optofluidic approaches for enhanced microsensor performances.* Sensors (Basel), 2015. **15**(1): p. 465-84.

44. Song, W. and J. Yang, *Optofluidic differential spectroscopy for absorbance detection of sub-nanolitre liquid samples.* Lab on a Chip, 2012. **12**(7): p. 1251-1254.

45. Wu, H., et al., *An ultra-low detection-limit optofluidic biosensor based on all glass Fabry-Perot cavity.* Optics Express, 2014. **22**(26): p. 31977-31983.

46. Chen, Y.-F., et al., *Optofluidic opportunities in global health, food, water and energy.* Nanoscale, 2012. **4**(16): p. 4839-4857.

47. Kiesel, P., M. Beck, and N. Johnson, *Monitoring CD4 in whole blood with an opto-fluidic detector based on spatially modulated fluorescence emission.* Cytometry Part A, 2011. **79**(4): p. 317-324.

48. Wu, S.H., et al., *Optofluidic Platform for Real-Time Monitoring of Live Cell Secretory Activities Using Fano Resonance in Gold Nanoslits.* Small, 2013. **9**(20): p. 3532-3540.

49. Nations, U., *Millennium Development Goals Reports.* United Nations Department of Economic and Social Affairs, 2014.

50. Breslauer, D.N., et al., *Mobile phone based clinical microscopy for global health applications.* PLoS One, 2009. **4**(7): p. e6320.

51. Zhu, H., et al., *Optofluidic fluorescent imaging cytometry on a cell phone.* Analytical Chemistry, 2011. **83**(17): p. 6641-6647.

52. Zhu, H. and A. Ozcan, *Wide-field fluorescent microscopy and fluorescent imaging flow cytometry on a cell-phone.* Journal of visualized experiments: JoVE, 2013(74).

53. Bishara, W., et al., *Lensfree on-chip microscopy over a wide field-of-view using pixel super-resolution.* Optics Express, 2010. **18**(11): p. 11181-11191.

54. Cui, X., et al., *Lensless high-resolution on-chip optofluidic microscopes for Caenorhabditis elegans and cell imaging.* Proceedings of the National Academy of Sciences, 2008. **105**(31): p. 10670-10675.

55. Zheng, G., et al., *Sub-pixel resolving optofluidic microscope for on-chip cell imaging.* Lab on a Chip, 2010. **10**(22): p. 3125-3129.

56. GENTAG, 2014.

57. Zhu, H., U. Sikora, and A. Ozcan, *Quantum dot enabled detection of Escherichia coli using a cell-phone.* Analyst, 2012. **137**(11): p. 2541-4.

58. Abkarian, M., et al., *Cellular-scale hydrodynamics.* Biomedical materials, 2008. **3**(3): p. 034011.

59. Wu, T.F. and Y.H. Lo, *Optofluidic device for label-free cell classification from whole blood.* Methods Mol Biol, 2015. **1256**: p. 191-200.

60. Thorsen, T., S.J. Maerkl, and S.R. Quake, *Microfluidic large-scale integration.* Science, 2002. **298**(5593): p. 580-584.

61. Sia, S.K. and G.M. Whitesides, *Microfluidic devices fabricated in poly (dimethylsiloxane) for biological studies.* Electrophoresis, 2003. **24**(21): p. 3563-3576.

62. Yager, P., et al., *Microfluidic diagnostic technologies for global public health.* Nature, 2006. **442**(7101): p. 412-418.

63. Trolio, W.M. and W.E. Coville, *Pre-Analytical Specimen Preparation.* Journal of the Association for Laboratory Automation, 2000. **5**(1): p. 72-78.

64. Brody, J.P., et al., *A planar microfabricated fluid filter.* Sensors and Actuators A: Physical, 1996. **54**(1): p. 704-708.

65. VanDelinder, V. and A. Groisman, *Separation of plasma from whole human blood in a continuous cross-flow in a molded microfluidic device.* Analytical chemistry, 2006. **78**(11): p. 3765-3771.

66. Crowley, T.A. and V. Pizziconi, *Isolation of plasma from whole blood using planar microfilters for lab-on-a-chip applications.* Lab on a Chip, 2005. **5**(9): p. 922-929.

67. Hou, H.W., et al., *Microfluidic devices for blood fractionation.* Micromachines, 2011. **2**(3): p. 319-343.

68. Lapizco-Encinas, B.H., et al., *An insulator-based (electrodeless) dielectrophoretic concentrator for microbes in water.* Journal of Microbiological methods, 2005. **62**(3): p. 317-326.

69. Ali, S., et al., *Characterization and feasibility of a miniaturized stirred tank bioreactor to perform E. coli high cell density fed-batch fermentations.* Biotechnology progress, 2012. **28**(1): p. 66-75.

70. Saunders, K.C., et al., *Separation and sample pre-treatment in bioanalysis using monolithic phases: A review.* Analytica chimica acta, 2009. **652**(1): p. 22-31.

71. Guirguis, R.A., *Liquid specimen container and attachable testing modules*. 2001, Google Patents.

72. Choi, S., et al., *Continuous blood cell separation by hydrophoretic filtration.* Lab on a Chip, 2007. **7**(11): p. 1532-1538.

73. Xuan, X., J. Zhu, and C. Church, *Particle focusing in microfluidic devices.* Microfluidics and nanofluidics, 2010. **9**(1): p. 1-16.

74. Tsutsui, H. and C.-M. Ho, *Cell separation by non-inertial force fields in microfluidic systems.* Mechanics research communications, 2009. **36**(1): p. 92-103.

75. Mohamed, H., et al., *Isolation of tumor cells using size and deformation.* Journal of Chromatography A, 2009. **1216**(47): p. 8289-8295.

76. Zheng, S., et al., *Membrane microfilter device for selective capture, electrolysis and genomic analysis of human circulating tumor cells.* Journal of Chromatography A, 2007. **1162**(2): p. 154-161.

77. Hosokawa, M., et al., *Size-selective microcavity array for rapid and efficient detection of circulating tumor cells.* Analytical chemistry, 2010. **82**(15): p. 6629-6635.

78. Tan, S.J., et al., *Microdevice for the isolation and enumeration of cancer cells from blood.* Biomedical microdevices, 2009. **11**(4): p. 883-892.

79. Wilf, M. and C. Bartels, *Optimization of seawater RO systems design.* Desalination, 2005. **173**(1): p. 1-12.

80. Yang, S.Y., et al., *Virus filtration membranes prepared from nanoporous block copolymers with good dimensional stability under high pressures and excellent solvent resistance.* Advanced Functional Materials, 2008. **18**(9): p. 1371-1377.

81. Hearn, M.T., et al., *Application of Reversed Phase High Performance Liquid Chromatography in Solid Phase Peptide Synthesis: High Pressure Liquid Chromatography of Amino Acids Peptides and Proteins XIII. Part XII Ref. 2.* Journal of Liquid Chromatography, 1979. **2**(1): p. 1-21.

82. de Mello, A.J. and N. Beard, *Focus. Dealing with 'real'samples: sample pre-treatment in microfluidic systems.* Lab on a Chip, 2003. **3**(1): p. 11N-20N.

83. Coville, W.E. and M. Loika, *Microfiltration Technology: A Sensible Approach to Automating Sample Preparation.* AMERICAN BIOTECHNOLOGY LABORATORY, 2006. **24**(8): p. 12.

84. Hamzah, A.A., et al., *Electrochemically deposited and etched membranes with precisely sized micropores for biological fluids microfiltration.* Journal of Micromechanics and Microengineering, 2013. **23**(7): p. 074007.

85. Li, S.J., C. Shen, and P.M. Sarro, *A Buried Vertical Filter for Micro and Nanoparticle Filtration.* Procedia Engineering, 2011. **25**(0): p. 1193-1196.

86. Van Rijn, C., et al., *Deflection and maximum load of microfiltration membrane sieves made with silicon micromachining.* Microelectromechanical Systems, Journal of, 1997. **6**(1): p. 48-54.

87. Tan, Swee Jin, et al. "Microdevice for the isolation and enumeration of cancer cells from blood." Biomedical microdevices 11.4 (2009): 883-892.

88. Krishnamurthy, S., et al., *Discordance in HER2 gene amplification in circulating and disseminated tumor cells in patients with operable breast cancer.* Cancer medicine, 2013. **2**(2): p. 226-233.

89. Mossoba, M., et al., *Application of a disposable transparent filtration membrane to the infrared spectroscopic discrimination among bacterial species.* Journal of microbiological methods, 2003. **55**(1): p. 311-314.

90. Wang, Y.-C., A.L. Stevens, and J. Han, *Million-fold preconcentration of proteins and peptides by nanofluidic filter.* Analytical chemistry, 2005. **77**(14): p. 4293-4299.

91. Mohamed, H., J.N. Turner, and M. Caggana, *Biochip for separating fetal cells from maternal circulation.* Journal of Chromatography A, 2007. **1162**(2): p. 187-192.

92. Lee, D., et al., *Separation of model mixtures of epsilon-globin positive fetal nucleated red blood cells and anucleate erythrocytes using a microfluidic device.* Journal of Chromatography A, 2010. **1217**(11): p. 1862-1866.

93. Huang, R., et al., *A microfluidics approach for the isolation of nucleated red blood cells (NRBCs) from the peripheral blood of pregnant women.* Prenatal diagnosis, 2008. **28**(10): p. 892-899.

94. Archibong, E., J. Stewart, and A. Pyayt, *Optofluidic spectroscopy integrated on optical fiber platform.* Sensing and Bio-Sensing Research, 2015. **3**(0): p. 1-6.

95. Parsons, G., J. Souk, and J. Batey, *Low hydrogen content stoichiometric silicon nitride films deposited by plasma-enhanced chemical vapor deposition.* Journal of applied physics, 1991. **70**(3): p. 1553-1560.

96. Williams, K.R. and R.S. Muller, *Etch rates for micromachining processing.* Microelectromechanical Systems, Journal of, 1996. **5**(4): p. 256-269.

97. Kohn, L.T., J. Corrigan, and M. Donaldson, *To err is human: Building a safer health system. Committee on Health Care in America. Institute of Medicine*. 1999, Washington (DC): National Academy Press.

98. Anderson, P. and T. Townsend, *Medication errors: Don't let them happen to you.* American Nurse Today, 2010. **5**(3): p. 23-27.

99. Linder, M.W. and P.E. Keck, *Standards of laboratory practice: antidepressant drug monitoring.* Clinical chemistry, 1998. **44**(5): p. 1073-1084.

100. Quiñones-Torrelo, C., et al., *Development of Predictive Retention−Activity Relationship Models of Tricyclic Antidepressants by Micellar Liquid Chromatography.* Journal of Medicinal Chemistry, 1999. **42**(16): p. 3154-3162.

101. Pankey, S., et al., *Quantitative homogeneous enzyme immunoassays for amitriptyline, nortriptyline, imipramine, and desipramine.* Clinical chemistry, 1986. **32**(5): p. 768-72.

102. Rao, M.L., et al., *Monitoring tricyclic antidepressant concentrations in serum by fluorescence polarization immunoassay compared with gas chromatography and HPLC.* Clinical chemistry, 1994. **40**(6): p. 929-33.

103. Myers, F.B. and L.P. Lee, *Innovations in optical microfluidic technologies for point-of-care diagnostics.* Lab on a Chip, 2008. **8**(12): p. 2015-2031.

104. Crismore, W.F., et al., *Electrochemical biosensor test strip*. 2001, Google Patents.

105. Fenton, E.M., et al., *Multiplex lateral-flow test strips fabricated by two-dimensional shaping.* ACS Appl Mater Interfaces, 2009. **1**(1): p. 124-9.

106. Martinez, A.W., S.T. Phillips, and G.M. Whitesides, *Three-dimensional microfluidic devices fabricated in layered paper and tape.* Proc Natl Acad Sci U S A, 2008. **105**(50): p. 19606-11.

107. Stone, H.A., A.D. Stroock, and A. Ajdari, *Engineering flows in small devices: microfluidics toward a lab-on-a-chip.* Annu. Rev. Fluid Mech., 2004. **36**: p. 381-411.

108. Jiang, H., X. Weng, and D. Li, *Microfluidic whole-blood immunoassays.* Microfluidics and nanofluidics, 2011. **10**(5): p. 941-964.

109. McNichols, R.J. and G.L. Cote, *Optical glucose sensing in biological fluids: an overview.* Journal of biomedical optics, 2000. **5**(1): p. 5-16.

110. Robinson, M.R., et al., *Noninvasive glucose monitoring in diabetic patients: a preliminary evaluation.* Clinical chemistry, 1992. **38**(9): p. 1618-1622.

111. Pyayt, A., et al. *Electro-optic polymer microring resonators made by photobleaching*. in *Integrated Optoelectronic Devices 2007*. 2007. International Society for Optics and Photonics.

112. Carlborg, C.F., et al., *A packaged optical slot-waveguide ring resonator sensor array for multiplex label-free assays in labs-on-chips.* Lab on a Chip, 2010. **10**(3): p. 281-290.

113. Sun, Y. and X. Fan, *Optical ring resonators for biochemical and chemical sensing.* Anal Bioanal Chem, 2011. **399**(1): p. 205-11.

114. Pyayt, A., et al. *Optical micro-resonator chemical sensor*. 2007.

115. Scullion, M., A. Di Falco, and T. Krauss, *Slotted photonic crystal cavities with integrated microfluidics for biosensing applications.* Biosensors and Bioelectronics, 2011. **27**(1): p. 101-105.

116. Fattal, D., et al. *Guided-mode resonance sensor with extended spatial sensitivity*. in *Optics East 2007*. 2007. International Society for Optics and Photonics.

117. Stewart, J. and A. Pyayt, *Photonic crystal based microscale flow cytometry.* Optics Express, 2014. **22**(11): p. 12853-12860.

118. Shopova, S., et al., *Plasmonic enhancement of a whispering-gallery-mode biosensor for single nanoparticle detection.* Applied Physics Letters, 2011. **98**(24): p. 243104.

119. Dantham, V., et al., *Taking whispering gallery-mode single virus detection and sizing to the limit.* Applied Physics Letters, 2012. **101**(4): p. 043704.

120. Holler, S., et al. *Label-free single cancer marker protein detection using a nanoplasmonic-photonic hybrid whispering gallery mode biosensor*. in *SPIE Sensing Technology+ Applications*. 2014. International Society for Optics and Photonics.

121. Liu, N., et al., *Infrared perfect absorber and its application as plasmonic sensor.* Nano letters, 2010. **10**(7): p. 2342-2348.

122. Kraner, J.C., et al., *Fatalities caused by the MDMA-related drug paramethoxyamphetamine (PMA).* Journal of analytical toxicology, 2001. **25**(7): p. 645-648.

123. Wielbo, D. and I.R. Tebbett, *The use of microcrystal tests in conjunction with Fourier transform infrared spectroscopy for the rapid identification of street drugs.* J Forensic Sci, 1992. **37**(4): p. 1134.

124. Wagner, H. and S. Bladt, *Plant drug analysis: a thin layer chromatography atlas*. 1996: Springer Science & Business Media.

125. Gaillard, Y. and G. Pépin, *Screening and identification of drugs in human hair by high-performance liquid chromatography—photodiode-array UV detection and gas chromatography—mass spectrometry after solid-phase extraction a powerful tool in forensic medicine.* Journal of Chromatography A, 1997. **762**(1): p. 251-267.

126. Weston, D.J., et al., *Direct analysis of pharmaceutical drug formulations using ion mobility spectrometry/quadrupole-time-of-flight mass spectrometry combined with desorption electrospray ionization.* Analytical chemistry, 2005. **77**(23): p. 7572-7580.

127. Maurin, J.K., et al., *The usefulness of simple X-ray powder diffraction analysis for counterfeit control—The Viagra® example.* Journal of pharmaceutical and biomedical analysis, 2007. **43**(4): p. 1514-1518.

128. S Coricone, B.M., N Ludwigsen, *Forensic Applications Of Vibrational Spectroscopy Techniques To Identify Prescription Drugs And Mixtures.* The Internet Journal of Forensic Science, 2011. **4**(2).

129. Scafi, S.H.F. and C. Pasquini, *Identification of counterfeit drugs using near-infrared spectroscopy.* Analyst, 2001. **126**(12): p. 2218-2224.

130. Holzgrabe, U., et al., *Quantitative NMR spectroscopy—applications in drug analysis.* Journal of pharmaceutical and biomedical analysis, 2005. **38**(5): p. 806-812.

131. Hargreaves, M.D., et al., *Analysis of seized drugs using portable Raman spectroscopy in an airport environment—a proof of principle study.* Journal of Raman Spectroscopy, 2008. **39**(7): p. 873-880.

132. Motz, J.T., et al., *Optical fiber probe for biomedical Raman spectroscopy.* Applied optics, 2004. **43**(3): p. 542-554.

133. Fujimoto, J.G., *Optical coherence tomography for ultrahigh resolution in vivo imaging.* Nature biotechnology, 2003. **21**(11): p. 1361-1367.

134. Li, M., et al., *Single cell Raman spectroscopy for cell sorting and imaging.* Current opinion in biotechnology, 2012. **23**(1): p. 56-63.

135. Myakov, A., et al., *Fiber optic probe for polarized reflectance spectroscopy in vivo: design and performance.* Journal of biomedical optics, 2002. **7**(3): p. 388-397.

136. Konorov, S.O., et al., *Hollow-core photonic crystal fiber-optic probes for Raman spectroscopy.* Optics letters, 2006. **31**(12): p. 1911-1913.

137. Nash, M.A., et al., *Multiplexed enrichment and detection of malarial biomarkers using a stimuli-responsive iron oxide and gold nanoparticle reagent system.* ACS Nano, 2012. **6**(8): p. 6776-85.

138. Kunda, S.G., Charles; Lynch, Sandra; Siegel, Neal *An Ultrasensitive Immunoassay Detection System for Biomarkers Utilizing Raman Scattering Methods.* AMERICAN LABORATORY, 2012.

139. Das, P., et al., *Designing a thiol specific fluorescent probe for possible use as a reagent for intracellular detection and estimation in blood serum: kinetic analysis to probe the role of intramolecular hydrogen bonding.* Organic & Biomolecular Chemistry, 2013. **11**(38): p. 6604-6614.

140. Kennedy, G., O. Buiu, and S. Taylor, *Oxidation of silicon nitride films in an oxygen plasma.* Journal of applied physics, 1999. **85**(6): p. 3319-3326.

141. Tong, H.D., et al., *Silicon nitride nanosieve membrane.* Nano letters, 2004. **4**(2): p. 283-287.

142. http://www.drugs.com/dosage/cyanocobalamin.html.

143. McGrath, J.K., P. Rankin, and M. Schendel, *Let the data speak: decreasing hemolysis rates through education, practice, and disclosure.* Journal of Emergency Nursing, 2012. **38**(3): p. 239-244.

144. Makroo, R.N., et al., *Evaluation of Red Cell Hemolysis in Packed Red Cells During Processing and Storage.* Apollo Medicine, 2010. **7**(1): p. 35-38.

145. Schaer, D.J., et al., *Hemolysis and free hemoglobin revisited: exploring hemoglobin and hemin scavengers as a novel class of therapeutic proteins.* Blood, 2013. **121**(8): p. 1276-1284.

146. Prahl, S., *Tabulated Molar Extinction Coefficient for Hemoglobin in Water.*

APPENDICES

Appendix A: Copyright Permissions

Below is permission for the use of materials in Chapter 4.

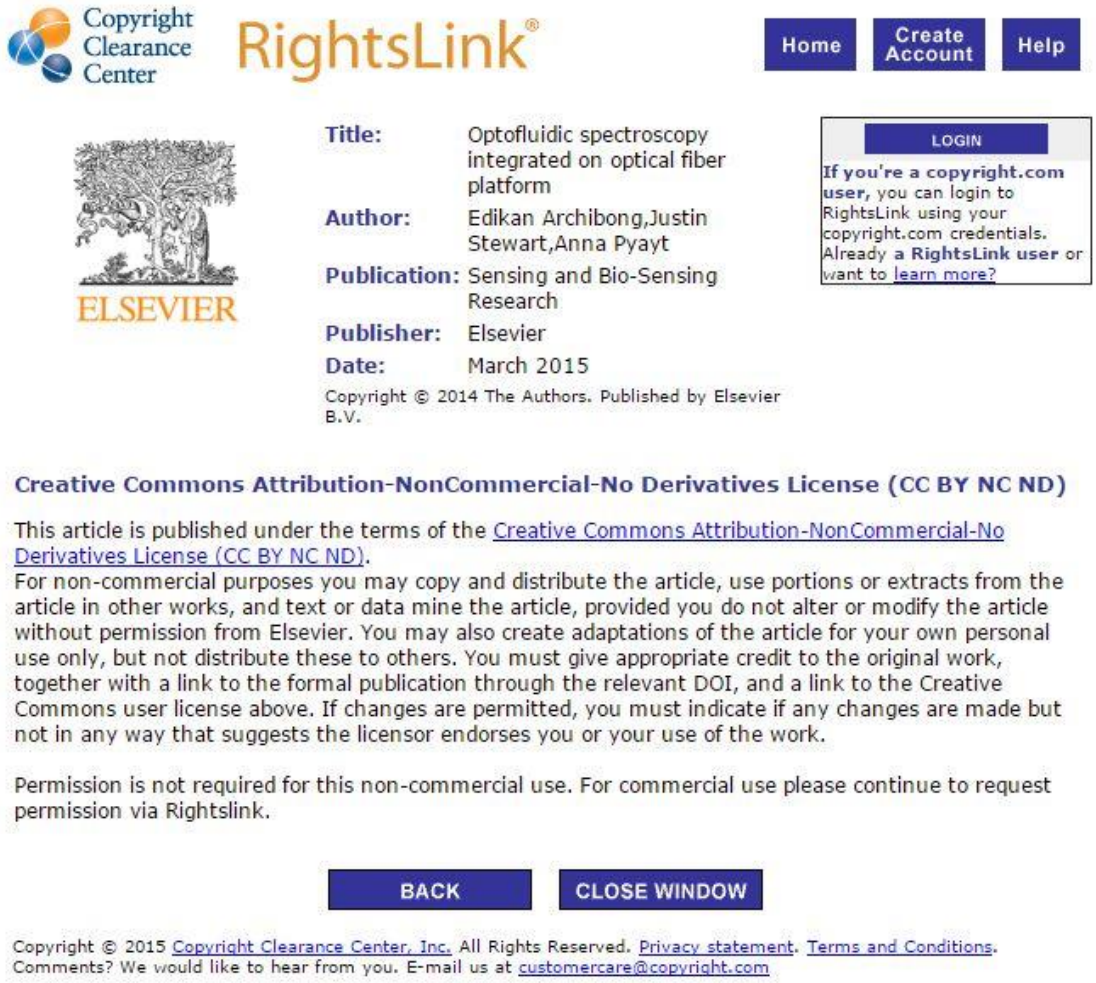

Copyright Clearance Center RightsLink®

Home | Create Account | Help

ELSEVIER

Title: Optofluidic spectroscopy integrated on optical fiber platform
Author: Edikan Archibong,Justin Stewart,Anna Pyayt
Publication: Sensing and Bio-Sensing Research
Publisher: Elsevier
Date: March 2015
Copyright © 2014 The Authors. Published by Elsevier B.V.

LOGIN

If you're a copyright.com user, you can login to RightsLink using your copyright.com credentials. Already a RightsLink user or want to learn more?

Creative Commons Attribution-NonCommercial-No Derivatives License (CC BY NC ND)

This article is published under the terms of the Creative Commons Attribution-NonCommercial-No Derivatives License (CC BY NC ND).
For non-commercial purposes you may copy and distribute the article, use portions or extracts from the article in other works, and text or data mine the article, provided you do not alter or modify the article without permission from Elsevier. You may also create adaptations of the article for your own personal use only, but not distribute these to others. You must give appropriate credit to the original work, together with a link to the formal publication through the relevant DOI, and a link to the Creative Commons user license above. If changes are permitted, you must indicate if any changes are made but not in any way that suggests the licensor endorses you or your use of the work.

Permission is not required for this non-commercial use. For commercial use please continue to request permission via Rightslink.

BACK | CLOSE WINDOW

Copyright © 2015 Copyright Clearance Center, Inc. All Rights Reserved. Privacy statement. Terms and Conditions.
Comments? We would like to hear from you. E-mail us at customercare@copyright.com

Edikan Archibong <earchibong@mail.usf.edu>

Image reprint

4 messages

Edikan Archibong <earchibong@mail.usf.edu> Wed, Oct 14, 2015 at 3:28 PM
To: glippi@ao.pr.it

Dear Dr. Lippi,

Hope this email finds you well. I have read a great deal about your work on hemolysis prevalance and would like to know if I can reproduce an image from your presentation (In vitro hemolysis: Causes, Prevalence, Effects, Measurement, and Solutions) for my dissertation

Thank you

--
Edikan Archibong, M.S.
Doctoral Student, Department of Chemical and Biomedical Engineering
University of South Florida
www.linkedin.com/in/Archibong

Edikan Archibong <earchibong@mail.usf.edu> Wed, Oct 14, 2015 at 3:55 PM
To: giuseppe.lippi@univr.it

Dear Dr. Lippi,

Hope this email finds you well. I would like to know if I can reproduce an image from your presentation (In vitro hemolysis: Causes, Prevalence, Effects, Measurement, and Solutions) for my dissertation

Thank you

[Quoted text hidden]

Prof. Giuseppe Lippi <giuseppe.lippi@univr.it> Wed, Oct 14, 2015 at 10:47 PM
To: Edikan Archibong <earchibong@mail.usf.edu>

Certainly!

best regards,

Giuseppe Lippi

Prof. Giuseppe Lippi
Full Professor of Clinical Biochemistry
Section of Clinical Biochemistry
University of Verona
Associate Editor of Clinical Chemistry and Laboratory Medicine
Associate Editor of Seminars in Thrombosis and Hemostasis
Tel. +39-045-8124308
E-mail: giuseppe.lippi@univr.it; ulippi@tin.it

----- Messaggio originale -----
Da: "Edikan Archibong" <earchibong@mail.usf.edu>
A: "giuseppe lippi" <giuseppe.lippi@univr.it>
Inviato: Mercoledì, 14 ottobre 2015 21:55:41
Oggetto: Fwd: Image reprint
[Quoted text hidden]

Edikan Archibong <earchibong@mail.usf.edu> Thu, Oct 15, 2015 at 12:10 AM
To: "Prof. Giuseppe Lippi" <giuseppe.lippi@univr.it>

Thank you Dr. Lippi
[Quoted text hidden]

ABOUT THE AUTHOR

Edikan Archibong was born in Akwa Ibom, Nigeria and immigrated to the U.S. at the age of 12. She obtained her B.S. in Chemistry in 2006 and M.S. in Analytical Chemistry in 2010, both from Florida A&M University (FAMU). Her thesis research was supported by the U.S. Dept. of Homeland Security Science & Technology Directorate and the National Center for Food Protection & Defense. At FAMU, she presented at national meetings organized by the American Chemical Society and National Organization of Black Chemists and Chemical Engineers. After completing her MS, Edikan enrolled in the Ph.D. program in Engineering Science within the Dept. of Chemical and Biomedical Engineering at the University of South Florida in 2011.

Edikan has been a student-leader of the National Organization of Black Chemists and Chemical Engineers with service on the 2011-2012 National Conference Planning Committee and planning the 2015 Annual Conference. In recognition of her career goals, research activities, involvement in K-12 STEM outreach and undergraduate mentoring, she was selected as recipient of the 2013 Winifred Burks-Houck Women's Graduate Student Leadership Award. Edikan's career goals include joining a federal research laboratory to investigate novel micro/nanotechnologies for early detection and treatment of diseases to improve clinical outcomes both in the U.S. and in low-resource countries, and developing biological and chemical countermeasures in advancement of national and homeland security.

Edikan is passionate about making a societial difference both in research toward the development of novel devices for point-of care diagnostics, and as a leader who will inspire the next generation of scientists from underrepresented backgrounds.